Solar Energy 237 (2022) 264–283

Contents lists available at ScienceDirect

Solar Energy

journal homepage: www.elsevier.com/locate/solener

Encapsulation of commercial and emerging solar cells with focus on perovskite solar cells

Kerttu Aitola [a,*], Gabriela Gava Sonai [b], Magnus Markkanen [a], Joice Jaqueline Kaschuk [c], Xuelan Hou [a], Kati Miettunen [b], Peter D. Lund [a,*]

[a] Aalto University School of Science, Department of Applied Physics, New Energy Technologies Group, Finland
[b] University of Turku, Faculty of Technology, Department of Mechanical and Materials Engineering, Finland
[c] Aalto University, School of Chemical Engineering, Department of Bioproducts and Biosystems, Finland

A B S T R A C T

Solar cell encapsulation literature is reviewed broadly in this paper. Commercial solar cells, such as silicon and thin film solar cells, are typically encapsulated with ethylene vinyl acetate polymer (EVA) layer and rigid layers (usually glass) and edge sealants. In our paper, we cover the encapsulation materials and methods of some emerging solar cell types, that is, those of the organic solar cells, the dye-sensitized solar cells and the perovskite solar cells, and we focus on the latter of the three as the newest contender in the solar cell arena. The PSC encapsulation literature is summarized in a comprehensive table we hope the reader may use as a "handbook" when designing encapsulation and long-term stability experiments. Some additional functionalities included in encapsulants are also discussed in our paper, e.g. improving the encapsulants' optical properties and manufacturing them sustainably from biobased materials.

1. Introduction

Photovoltaics (PV) is a rapidly growing energy production method, that amounted to around 2.2% of global electricity production in 2019 (Photovoltaics Report - Fraunhofer ISE, 2020). Crystalline silicon solar cells dominate the commercial PV market sovereignly: 95% of commercially produced cells and panels were multi- and mono-crystalline silicon, and the remaining 5% were cadmium telluride (CdTe), copper indium gallium selenide (CIGS) and amorphous silicon (a-Si) (Photovoltaics Report - Fraunhofer ISE, 2020). Contenders to the aforementioned commercial solar cells are for instance organic solar cells (OSC), dye-sensitized solar cells (DSSC) and perovskite solar cells (PSC), or so-called emerging photovoltaic techniques, even though it may be challenging for the other technologies to compete with the peak Watt price of mainstream crystalline silicon PV modules, that is presently (April 2021) in the 0.2 $ range (Schachinger, 2021). However, there is academic and commercial interest to develop the emerging PV technologies for different application areas where the commercial cells are not utilized: for instance, the DSC is considered being a good option for indoor PV applications (Lan et al., 2012), and the PSC is envisioned to be a good choice for tandem devices with Silicon, because its bandgap is tunable and can be complementary to that of silicon solar cells (Jacobsson et al., 2016).

Solar cell (and panel) encapsulation is a critical issue for the good long-term performance of those devices. In principle, most active materials in solar cell are sensitive to e.g. ambient oxygen and moisture, UV radiation, heat, and even mechanical threats from the environment, and the active layers need to be protected from those phenomena with suitable encapsulation. In addition to the protection functionality, solar cell encapsulation materials need to be transparent on the solar cell side where light is incident on the solar cells. They need to be low cost and industrially viable, and sometimes flexibility is a desired property. They must handle the environmental stresses mentioned above and reach long-term stability preferably for over 20-year time periods.

Encapsulation has often a direct link to solar cell stability. The most relevant industrial stability standards for PV modules are issued by the International Electrotechnical Commission (IEC) and have been summarized in the IEC 61251 standard that entails several detailed and interconnected accelerated aging tests (Holzhey and Saliba, 2018). Crystalline silicon modules pass these tests and have shown to offer 25–30 year stabilities (Wilson et al., 2020). It can be assumed that PSCs and other emerging PV technologies need to pass these tests too, in order to fulfill the requirements of commercialization and large-scale use. However, it has been pointed out that the IEC aging tests may not be suitable for emerging PV technologies since their degradation mechanisms are most likely different from those of silicon PV (Khenkin et al., 2020). Therefore, PSCs may need to be subject to a modified set of aging tests, accounting also for PSC specific degradation phenomena,

* Corresponding authors.
E-mail addresses: kerttu.aitola@aalto.fi (K. Aitola), peter.lund@aalto.fi (P.D. Lund).

https://doi.org/10.1016/j.solener.2022.03.060
Received 13 April 2021; Received in revised form 4 October 2021; Accepted 22 March 2022
Available online 8 April 2022

originally proposed at the International Summit of Organic PV stability (ISOS) in 2011 for OPV cells. The set of stability testing protocols has been published as article "Consensus statement for stability assessment and reporting for perovskite photovoltaics based on ISOS procedures" (Khenkin et al., 2020). The unique PSC degradation phenomena could also affect the encapsulation approaches used with the technology.

In this paper, we review the literature on the encapsulation of commercial solar cells (Si, CdTe, CIGS, a-Si) and some emerging PV technologies, namely the PSC, DSSC and OSC. We hope that this review can provide a reference source for improved designing, utilizing, and developing of solar cell encapsulation of especially PSCs, as the newest contender in the field.

2. Functionalities linked to solar cell encapsulation

In the "Consensus statement for stability assessment and reporting for perovskite photovoltaics based on ISOS procedures", [PSC] encapsulation is defined as the protection of solar cells by gas-barrier materials that "delays contact between the cell and ambient air (especially moisture)" (Khenkin et al., 2020). As types of different encapsulation methods/configurations, the authors list glass-glass encapsulation, lamination of rigid or flexible materials, direct deposition, or a combination of these. The authors do not include "stress tests specific to encapsulated modules", such as hail tests and potential induced degradation, in their consensus statement, and state that these might be leveraged from the existing IEC 61215 standard in the future.

In general, there are several functionalities that are required from solar cell (PV module) encapsulation materials. According to Hasan et al., an encapsulant should provide protection toward moisture and other foreign impurities, as well as fortification from mechanical damage, and it should also act as an electrical insulator between the cells, the interconnects and the other module components, and bind the cell components together (Hasan and Arif, 2014). In addition to those properties, there are several other ones, of which some are obvious, such as transparency (>90%) on the side where the light is incident on the solar cell, chemical inertness toward the solar cell active materials, good adherence on the substrate, cost-effectiveness, industrial viability, mechanical durability toward mechanical environmental threats e.g. hail storms, and stability at high temperatures of >80 °C and high light intensities, including UV light. Some encapsulation requirements on the other hand are less obvious and they are addressed in the following. Some desired properties are for instance high dielectric breakdown (the electrical breakdown voltage for the insulator), high volume resistivity (term describing the electrical resistivity of a plastic material), and matching refractive index with the solar cell active materials (Aristidou et al., 2015). The encapsulant material must have suitable thermal expansion properties. Its oxygen transmission rate (OTR) and water vapor transmission rate (WVTR), that represent the rates at which oxygen and water vapor, respectively, are transmitted through the encapsulant material, must be adequately low. Jakaria et al. listed OPV encapsulation material requirements that are summarized in Table 1 (Ahmad et al., 2013).

3. Perovskite solar cells

Perovskite solar cell (PSC) is an emerging photovoltaic technology with a striking 25.5% laboratory scale power conversion efficiency (PCE) (NREL, 2020), that has been achieved in less than ten years of research (Jeon et al., 2015; Lee et al., 2012; NREL, 2020). The "perovskite" refers to the hybrid organic–inorganic perovskite absorbers with the perovskite crystal structure ABX_3, where A is typically methylammonium (MA^+), formamidinium (FA^+) or Cs^+ anion, B is Pb^{2+} cation, and X is I^-, Br^- or Cl^- anion. The perovskite absorber has most commonly an octahedral lead halide (PbX_6) scaffold with the organic or Cs^+ cations occupying the "interstitial" space, with the tetragonal crystal structure being the most optimal from the photovoltaic point of view, see Fig. 1.

Table 1
Specifications and requirements for OPV encapsulant materials. Reprinted from Ref (Ahmad et al., 2013).

Characteristics	Specification or requirement
WVTR	10^{-4}–10^{-6} g m^{-2} day^{-1}
OTR	10^{-3}–10^{-5} cm^3 m^{-2} day^{-1} atm^{-1}
Glass transition temperature (T_g)	<−40 °C (during winter in deserts)
Total hemispherical light transmission over the wavelength range from 400 nm to 1100 nm	> 90% of incident light
Hydrolysis	None (80 °C, 100% RH)
Water absorption	< 0.5 wt% (20 °C/100% RH)
Resistance to thermal oxidation	Stable (up to 85 °C)
Mechanical creep	None (90 °C)
Tensile modulus	< 20.7 MPa (<3000 psi) at 25 °C
Chemical inertness	No reaction (with embedded Cu coupons at 90 °C)
UV absorption degradation	None (>350 nm)
Hazing or clouding	None (80 °C, 100% RH)

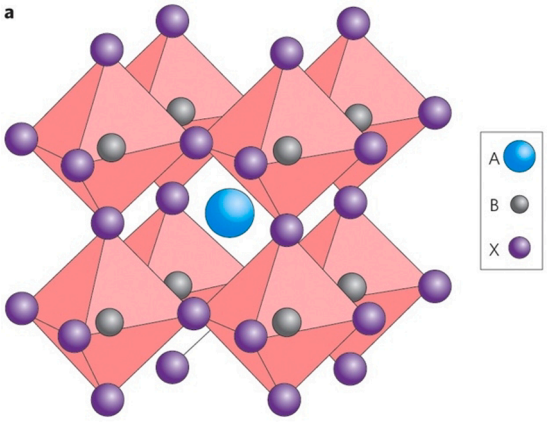

Fig. 1. The octahedral perovskite crystal structure. Reprinted from Ref (Green et al., 2014). (For interpretation of the references to color in this figure legend, the reader is referred to the web version of this article.)

The original breakthrough research published in 2012 was carried out with the methylammonium lead iodide ($MAPbI_3$) perovskite absorber, combined with a mesoporous TiO_2 electron contact and a 2,2′,7,7′-tetrakis(N,N-di-4-methoxyphenylamino)-9,9′-spirobifluorene (Spiro-OMeTAD) hole contact (Kim et al., 2012; Lee et al., 2012), but since then several other perovskite compositions and contact materials have been suggested, that are discussed in the following chapter. The perovskite absorbers employed in the solar cells have several attractive optoelectronic properties. They exhibit optimal and tunable band gaps to the solar spectrum, high absorption coefficients, long electron diffusion lengths (over 1 um), high charge mobilities, meaning that thin films (in the 100 nm thickness range) can be utilized in the cells and low exciton binding energies (Roy et al., 2020). The PSC is also based on very cost-effective starting materials, it can be manufactured with low-temperature liquid processes that could be upscaled easily to industrial scale processes, and it can be prepared flexible, which offers industrial advantages, such as possibilities for roll-to-roll production and several application areas, e.g. in building integration and in portable, lightweight energy sources. There are downsides to the technology too: the perovskite absorbers are quite sensitive toward e.g. atmospheric water and oxygen and lead is a toxin whose industrial handling is problematic, even though the amount utilized in an individual cell is small (few hundred milligrams in a square meter of a solar panel) (Babayigit et al., 2016).

The original PSC stack consisted of FTO glass/dense TiO_2/mesoporous TiO_2/$MAPbI_3$/Spiro-OMeTAD/metal contact layers (the so-called "nip" structure, shown in Fig. 2) but different "mixed"

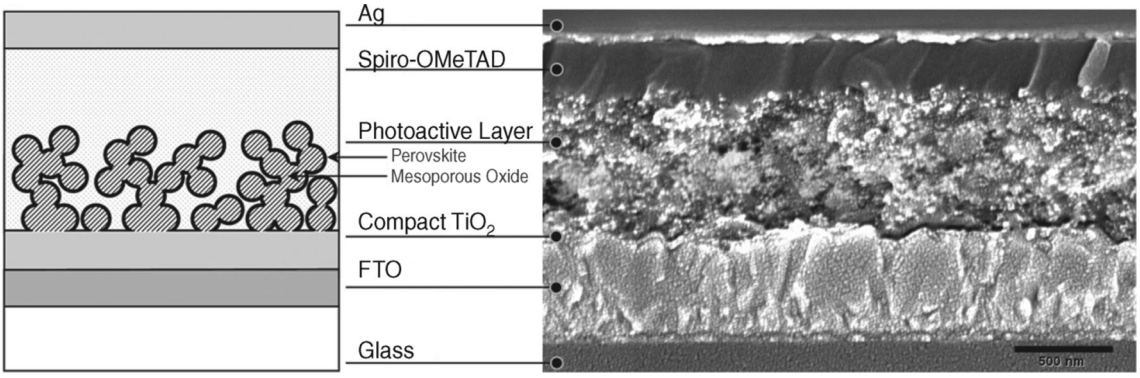

Fig. 2. The original PSC stack with $MAPbI_3$ perovskite light absorber and its electron micrograph, reprinted from (Lee et al., 2012).

perovskite composite formulations have been used, such as formamidinium lead iodide:methylammonium lead bromide $(FAPbI_3)_{0.85}$-$MAPbBr_3)_{0.15}$ compositions (Jeon et al., 2015; Pellet et al., 2014), $Cs_{0.5}(MA_{0.17}FA_{0.83})_{0.95}Pb(I_{0.83}Br_{0.17})_3$ (Michael Saliba et al., 2016) and the Rb-containing version of the latter (M. Saliba et al., 2016), that have better light absorption and long-term stability properties than the $MAPbI_3$ perovskite. $Cs_{0.17}FA_{0.83}PbI_{0.83}Br_{0.17}$ has been proposed to be suitable for PSC-SSC tandems with its bandgap of 1.63 eV and even more stable than the aforementioned perovskites (Kamino et al., 2019), and the recent ultrahigh published PSC PCE of 24.8% was obtained with MACl-stabilized $FAPbI_3$ (Jeong et al., 2020; M. Kim et al., 2019) – results that elucidate that scientific consensus on the "best" perovskite composition is yet to be achieved. In addition to the nip structure with the mesoporous TiO_2 contact, the PSCs can be manufactured with mesoporous non-conducting Al_2O_3 "scaffold" layer on a dense TiO_2 layer (Zhang et al., 2015), and in the so called "planar" configuration with planar bottom contact layers such as SnO_2 (Jiang et al., 2018). Also planar "pin" structures (e.g. NiOx/$MAPbI_3$/fullerene configuration) have been suggested (Jeng et al., 2014).

Several alternative contact materials to TiO_2 and Spiro-OMeTAD have been successfully employed, such as solution processed SnO_2 (Jiang et al., 2018), evaporated fullerenes (Wojciechowski et al., 2015a), and fullerene derivatives such as [6,6]- phenyl C_{61}-butyric acid methyl ester (PCBM) as alternative electron-selective contacts, and NiOx (Jeng et al., 2014), poly(triaryl)amine polymer (M. Saliba et al., 2016) and self-assembled molecular layers (e.g. ([2-(9H-carbazol-9-yl)ethyl] phosphonic acid)) (Al-Ashouri et al., 2019) as hole-selective contacts. Lead-free perovskites based on tin (Shao et al., 2018) and bismuth (Park et al., 2015) have been reported, but with lower efficiencies and stabilities than the Pb-based perovskites.

The perovskite layer is typically manufactured via a one-step solvent engineering process (Jeon et al., 2014), where the precursor solution is first spin coated on the TCO glass substrate and so-called antisolvent is applied on the spinning precursor layer, resulting in an "intermediate phase" perovskite layer, followed by annealing at around 100 °C, that yields the final photoactive perovskite phase. Also 2-step methods are widely employed, in which a PbI_2 film is in dipped in a MAI solution and annealed thereafter (Bi et al., 2014). Up-scalable manufacturing methods such as slot die coating (Vijayan et al., 2020), blade coating (Vijayan et al., 2020) and evaporation (Liu et al., 2013) have been demonstrated.

3.1. *Stability issues of perovskite solar cells*

PSC stability has been considered to being one of the greatest hurdles that must be overcome before commercialization the solar cell type. There are several complex stability issues related to the solar cell type, of which some are presented in this chapter.

One of the main PSC stability issues is perovskite absorber instability toward ambient water vapor (Yang et al., 2015): when $MAPbI_3$ perovskite is exposed to water vapor it decomposes into PbI_2 and MAI. On the other hand, also oxygen vapor combined with light is harmful to the $MAPbI_3$ perovskite (superoxide O_2^- is created when photoexcited electrons in the perovskite interact with molecular oxygen, and the superoxide reacts with the methylammonium moiety in the perovskite, causing decomposition and degradation) (Aristidou et al., 2015). $MAPbI_3$ perovskite undergoes an undesired tetragonal-to-cubic phase transition at around 55 °C (Baikie et al., 2013), which affects its light absorption adversely, and it is chemically unstable at temperatures of around 85 °C, due to MA ion volatility (Conings et al., 2015; Dualeh et al., 2014). It has however been found that the so called "mixed ion perovskites", such as $(FAPbI_3)_{0.85}MAPbBr_3)_{0.15}$ (Jeon et al., 2015; Pellet et al., 2014), and the Cs- (Michael Saliba et al., 2016) and Rb-containing (M. Saliba et al., 2016) versions of it, are more stable toward high temperature effects owing to the so-called entropy of mixing.

It has also been observed that ion (iodide vacancy) migration in a functioning PSC causes not only undesired hysteretic IV performance but also erosion of the perovskite crystal in the long run and therefore perovskite film defect management is of utmost importance from long-term stability point of view (Lee et al., 2019). On the other hand, photoinstability of e.g. the mixed perovskite $MAPb(Br_xI_{(1-x)})_3$ results in reversible creation of iodide rich domains (Hoke et al., 2015), whose long-term behavior in a solar cell is however unknown.

Another stability touching stone has been the PSC selective contact materials. The ubiquitously utilized Spiro-OMeTAD forms unwanted, large crystalline domains at over 60 °C temperatures (Malinauskas et al., 2015; Matteocci et al., 2016) and allows ions from the metal contact to migrate through the cell, rendering it un-operational (Domanski et al., 2016). On the other hand, the "standard" electron contact TiO_2 is photocatalytic under UV light, which has been suggested to cause stability issues for PSCs (Leijtens et al., 2013). You et al. proposed that the electron contact SnO_2 offers improved stability compared to TiO_2; even though SnO_2 is also photocatalytic (to a lower degree than TiO_2), and indeed better PSC stabilities have been reported with the contact material (Jiang et al., 2018). The conductive polymer poly(triaryl amine yielded impressive stability results when combined with Rb-containing perovskites (M. Saliba et al., 2016), as well as the inorganic hole conductor CuSCN (Habisreutinger et al., 2014a). Different carbon nanomaterials such as fullerenes (Wojciechowski et al., 2015b), carbon black (Baranwal et al., 2019; Li et al., 2015; Rajamanickam et al., 2016), and carbon nanotubes (Aitola et al., 2017; Habisreutinger et al., 2014a) have yielded good stability results. TiO_2 and Spiro-OMeTAD contacts have however produced some of the highest PCEs to date, meaning replacing them in the high PCE PSCs requires more research on the contact materials. The recently published 24.8% PCE was obtained with hydrophobic, fluorinated Spiro-OMeTAD derivatives, that resulted in 50% RH "storage" test of un-encapsulated cells, compared to the stabilities of the cells with Spiro-OMeTAD contacts (Jeong et al., 2020).

4. Encapsulation of commercial solar cells

4.1. Silicon solar cell encapsulation

Crystalline silicon PV modules are typically encapsulated via sandwiching the cells between a top glass sheet and a polymeric encapsulant layer, and a second layer of encapsulant and a polymeric backsheet, see Fig. 3a) for a schematic image. Fig. 3 depicts also the substrate (a) and superstrate-type (b) of thin film solar cell encapsulation and manufacturing schemes, that are discussed in Chapter 4.2. In addition, a polyisobutylene edge sealant (Lange et al., 2011) and an aluminum frame is applied around the module (Cattaneo et al., 2014). Currently the most common polymeric encapsulant material in commercial silicon solar modules is ethylene–vinyl acetate (EVA) (Kempe, 2011; Peike et al., 2013). EVA is applied to a silicon module as a film via a lamination process that consists of three main steps: 1) heating the encapsulant homogeneously to ensure homogeneous curing of the encapsulant, 2) applying vacuum to remove air bubbles and unwanted impurities, and 3) applying pressure to ensure proper surface contact and adhesion between the encapsulant and other parts of the module. All of the 3 steps are carried out with different temperature, pressure and time, that may affect the properties of the PV module, and therefore finding optimal applying parameters for each encapsulant is crucial for PV module manufacturers (Lange et al., 2011).

EVA was originally chosen as the encapsulant material for commercial solar modules due to its adequate chemical and physical properties relative to low cost and good processability (Czanderna and Pern, 1996). Since cost is a key factor in photovoltaic systems and their real life applications, it is very challenging for an alternative material to replace EVA as the “standard” encapsulant (Goodrich et al., 2013). EVA however has multiple negative properties. For instance, it is prone to discoloring (turning yellow/brown) resulting in decreased light-transmittance, and therefore reduced solar cell power output (Czanderna and Pern, 1996; Rajput et al., 2019). Its water vapor transmission rate (WVTR) is rather low compared to that of some other proposed encapsulants (Cattaneo et al., 2014), but on the other hand, its water diffusion rate is high, causing potentially significant degradation over module lifetime (Kempe, 2006). One EVA degradation mechanism is the decomposition of the vinyl acetate (VA) group of the polymer into acetic acid, resulting in discoloration (Adothu et al., 2019; Cattaneo et al., 2014; Czanderna and Pern, 1996; Patel et al., 2020), that may happen when EVA is exposed to water or UV-radiation (Cattaneo et al., 2014; Czanderna and Pern, 1996). The resulting acetic acid may also cause electrical contact corrosion (Kraft et al., 2015). Besides causing EVA decomposition, water ingress degrades the solar module by causing delamination and corrosion on the metallic contacts (Dechthummarong et al., 2010). Poor adhesion of the encapsulant has been reported to increase the water ingress of the encapsulant (Adothu et al., 2019; Kempe, 2011). A recently recognized failure mode of PV modules is the potential induced degradation (PID), that appears as leakage current through the encapsulant and the glass substrate/superstrate, because of a potential difference between the solar cells and the grounded metallic frame of the PV module. Due to the increasing system sizes, PID has become a significant failure mode of PV modules and the electrical resistivity of the encapsulant has become ever more important.(López-Escalante et al., 2016) It has been speculated that PID has always been a form of degradation, but only with modern measurement technology it has been noticed.

The aforementioned negative qualities of EVA have been overcome by using additives, such as UV absorbers and adhesion promoters, but these additives can also degrade and cause further degradation of the solar module, such as encapsulant discoloring and delamination (Adothu et al., 2019; Czanderna and Pern, 1996). A polymer crosslinker can be added to the encapsulant in order to increase its adhesion on the silicon layer. Crosslinking is generally thought to increase the quality of the encapsulant, but during the crosslinking unwanted byproducts can be formed into the encapsulation layer (Adothu et al., 2019). These impurities can cause defects in the encapsulant, that reduce the PCE and/or the lifetime of the module. The crosslinker should be activated either thermally, chemically or with UV light. The activation of the crosslinker causes an extra step in the manufacturing process that adds to the production costs of the PV modules. Often the used crosslinker is thermally activated in temperatures greater than the melting point of the encapsulant (Gawlińska et al., 2018; Hirschl et al., 2013), that can cause cracking and displacement of the cells due to mismatch of the thermal expansion coefficient between the cell and the super- or the substrate (Dietrich et al., 2010).

Before EVA became the dominant encapsulant, polyvinyl butyral (PVB) and polydimethylsiloxane (PDMS) were commonly used as silicon solar panel encapsulants (Czanderna and Pern, 1996; Kempe, 2011). In terms of properties, PVB has some clear advantages over EVA, such as good adhesion without crosslinking and fast processing time (Peike et al., 2013). Disadvantages of PVB include high water vapor transmission and absorption rates and poor electrical resistivity (called typically “volume resistivity” in this context) (Kempe, 2011; Swonke and Auer, 2009). PVB has roughly 100 times smaller volume resistivity than EVA and the resistivity is decreased even further when PVB has absorbed water (Kempe, 2011). PVB has also been reported to degrade faster than EVA during accelerated UV aging (Kempe et al., 2009). Recently, PVB has however emerged once again as a potential encapsulant due to its good UV light transparency and better UV light stability compared to that of EVA’s (Peike et al., 2013) and relatively low cost. Since PVB has high WVTR, the used sub- and superstrates of the PV module need to exhibit good resistance against moisture ingress to

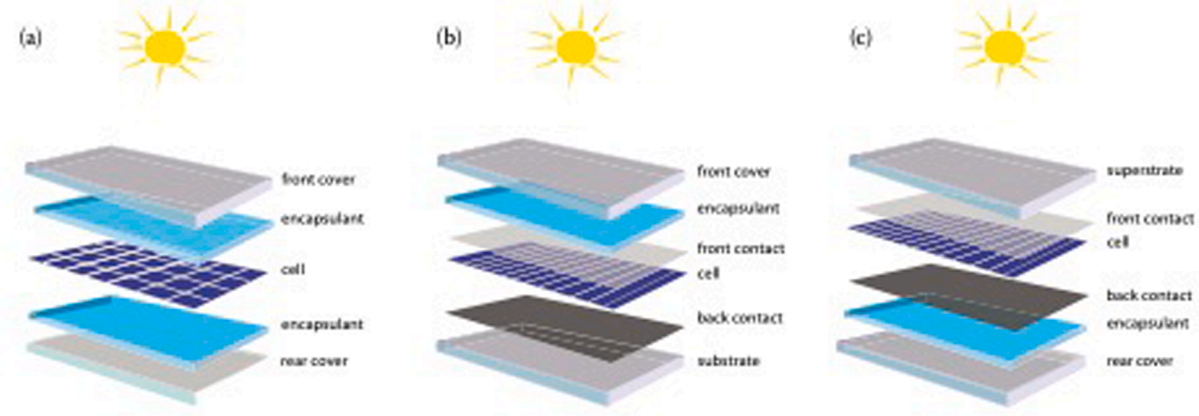

Fig. 3. Schematic image of a) silicon PV module encapsulation, b) substrate type thin film PV module encapsulation, and superstrate-type thin film PV module encapsulation, reprinted from (Peike et al., 2013).

compensate for this weakness. PVB is the second most used encapsulation material in PV modules (Peike et al., 2013) and it is commonly used commercially in building integrated photovoltaics, such as solar windows and facades (Cattaneo et al., 2014; Yang et al., 2017).

PDMS was one of the first encapsulation materials used for PV modules (Kempe, 2011). PDMS and other silicon based encapsulants have interesting properties as an encapsulation layer (see below), although the price of these encapsulants is noticeably higher than that of other encapsulants, such as EVA and PVB (Hasan and Arif, 2014). PDMS encapsulants have been reported to withstand UV radiation with minimal losses in light transmittance (Kempe et al., 2009), because the polymer chain contains Si-O bonds that are a main factor in the UV resistance of these encapsulants (Kempe, 2011). Light transmittance of PDMS is also generally higher compared to that of other commercial encapsulants. This is partially due to the fact that PDMS does not need additional UV absorbers, since decomposition of bonds due to UV irradiance is not common for PDMS (Kempe, 2011). PDMS-based encapsulants require however crosslinking to ensure good adhesion on a substrate. Even though the crosslinking process can cause unwanted impurities in the encapsulation layer, crosslinking creates chemical bonds that are more resistant against humidity (Kempe, 2011). In principle PDMS has a high WVTR compared to the other encapsulants, but because it is a hydrophobic material, the amount of water absorbed in practice is low (Swonke and Auer, 2009).The downsides of PDMS are high cost and relatively difficult processing. Unlike the other encapsulants discussed here, PDMS is applied as a two-part resin rather than a foil, and because of this, PDMS-based encapsulants require special equipment, meaning additional investments in the PV production line.

A fairly new candidate to replace EVA is thermoplastic polyolefin (TPO). TPO adheres well on many different substrates without crosslinking, meaning low production costs and eliminating potential byproducts caused by a crosslinking process (Adothu et al., 2019; Kempe, 2011; López-Escalante et al., 2016). TPO has also been reported being very resistant toward creep, which is a common failure mode for thermoplastic (non-crosslinking) encapsulants (Kempe et al., 2016; Miller et al., 2010). Also, TPO conserves its light transmittance better than EVA during light exposure (López-Escalante et al., 2016), and its discoloration rate is around nine times slower than EVA when exposed to UV radiation (Adothu et al., 2019). TPO has low WVTR relative to other potential encapsulation materials and its volume resistivity is very high (López-Escalante et al., 2016). Its price and lamination procedure are similar to that of EVA's (Adothu et al., 2019), meaning that no large investments in production facilities would be required in order to switch to TPO (López-Escalante et al., 2016), and therefore TPO has seen a lot of academic interest in the past years.

A rare but cost-efficient encapsulant material for PV modules is thermoplastic polyurethane (TPU). TPU is generally applied without a crosslinker, but it suffers from creep and displacement when compared to the other non-crosslinking encapsulants (Miller et al., 2010). This could be overcome by introducing a crosslinker to the encapsulant, however, one of the major advantages of TPU over EVA is the elimination of the crosslinker. The TPU monomer contains an ester bond that is hydrolytically unstable and the breaking this bond leads to a decrease of viscosity, that in return can cause delamination and creep of the encapsulant (Kempe, 2011). TPU has similar light transmittance and degradation rate as EVA and both of these materials have similar volume resistivity (Kempe, 2011; Kempe et al., 2009). Since TPU does not have any significant advantage over EVA, TPU is not a very likely candidate to replace EVA as the dominant encapsulation material for commercial PV modules.

Another group of encapsulation materials in the photovoltaic industry are ionomers. Especially ethylene ionomers exhibit properties that are suitable for encapsulating PV modules: ionomers are able to withstand thermal and UV stress and their volume resistivity is high (Cattaneo et al., 2014). Their WVTR is very low (Nagayama et al., 2020) and they are typically employed without a crosslinker. Their light transmittance is also very high and their discoloring rate is lower compared to that of the other common encapsulation materials, such as EVA's (Tracy et al., 2020). On paper, ionomers may seem like an ideal candidate for an encapsulation material, but since they are not commonly used in PV applications, research on their durability is lacking. According to a recent study, the adhesion energy of ionomers decreases quickly when exposed to UV radiation (EVA had twice as large adhesion energy as the used ionomers before aging) (Tracy et al., 2020). Currently ionomers are also a relatively expensive option for an encapsulation material and PV modules encapsulated with them would have to have exceptional durability in order to compete in the industry (Hasan and Arif, 2014). Nonetheless, academic interest on ionomer encapsulants has increased in the recent years (Hasan and Arif, 2014; Tracy et al., 2020).

The main observations from silicon PV module encapsulation include:

- EVA and glass are industrially established encapsulation materials that are applied with a lamination procedure utilizing heat, vacuum and pressure;
- TPO is an interesting and cost-efficient alternative to EVA;
- PDMS and ionomers are promising but so far expensive options.

4.2. Thin film solar cell encapsulation

Thin film solar cells are an established alternative PV technology, the most important of those being cadmium telluride, copper indium gallium diselenide and amorphous silicon (a-Si:H). In 2019 the global installations of thin film solar cells amounted to 5.7 GW_p for CdTe, 1.6 GW_p for CIGS and 0.2 GW_p for a-Si (out of a 5% total PV market share) (Photovoltaics Report - Fraunhofer ISE, 2020). Thin film technologies allow manufacturing of flexible cells, but flexible cell types have not yet gained a lot of commercial popularity. All the above mentioned three thin film solar cell types are, as silicon solar cells, usually encapsulated with EVA and glass back- or frontsheets, but alternative methods have also been suggested.

CdTe solar cells, that dominate the thin film market, are typically manufactured on a TCO glass superstrate via a vapor transport procedure and they are typically encapsulated with EVA and a glass backsheet, resulting in glass-glass encapsulation (Fig. 3c) (Fthenakis et al., 2020). Some alternative encapsulation methods have been demonstrated. For instance CdTe cells with a multilayer encapsulant comprising of sputtered oxide and acrylate-based polymer survived a 1000 hr 60 °C/90% RH damp-heat test in environmental chamber, with a 15% drop in PCE (it should be mentioned that CIGS solar cells, that were also included in the study, fared better in the same test) (Olsen et al., 2005). Luminescent down-shifting dyes incorporated in the EVA layer covered with a fluorinated ethylene propylene (FEP) front sheet was shown to improve CdTe cells' short-circuit current (Parel et al., 2015; Ross et al., 2014), see Fig. 4 for a schematic of a CdTe cell in which the FEP layer was employed

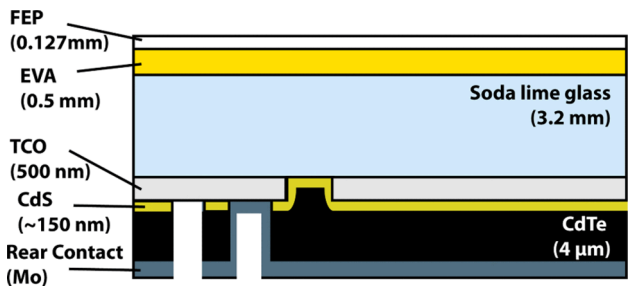

Fig. 4. A schematic image of an CdTe cell encapsulation concept, in which luminescent the EVA layer is doped with luminescent down-shifting dyes and fluorinated ethylene propylene sheet is used as the front cover, reprinted from (Parel et al., 2015; Ross et al., 2014).

in place of the typical front glass sheet. It was also found, that in the case of a fire, the resulting molten glass matrix contained most of the toxic Cd (99.5%) and prevented its leak to the environment, meaning that glass-glass-encapsulation is a good option with toxic solar cell materials from fire safety point of view (Fthenakis et al., 2005).

CIGS solar cells are usually manufactured by sputtering or evaporation on a glass substrate and the cells are normally encapsulated with EVA and a glass frontsheet (Fig. 3b). It has been observed that EVA causes compressive stress on the CIGS cell due to EVA's thermal expansion in the lamination process, depending on the EVA gel content (cross linking), that on the other hand depends on the temperature and the pressure in the lamination process, causing PCE loss (Xu, 2017). CIGC cells with a Tedlar/PET/Al foil/Tedlar backsheet with 0.001 g m^{-2} d^{-1} WVTR performed as well as EVA and glass backsheet-encapsulated cells in a 50 h 85 °C/85% RH damp-heat aging test, in a comparative study conducted with different polymer backsheets (Sundaramoorthy et al., 2010). A 55 nm thick ALD-grown Al_2O_3/epoxy/Teflon structure was found to function as well as epoxy and glass backsheet in a combined 1000 h 85 °C/85% RH and light soaking test, with only a minor drop in cell PCE for both encapsulation types (Carcia et al., 2010). Flexible CIGS cells with a flexible multilayer AlOx and unnamed polymer on PET/PEN substrate encapsulant laminated on both sides of the cell survived a damp heat test 85 °C/85 %RH with less than a 10% drop in PCE (Olsen et al., 2008).

EVA and glass backsheets are also the most typical lamination materials of rigid a-Si cells manufactured typically via chemical vapor deposition on a glass substrates (Fig. 3b) (Arya and Carlson, 2002; Green, 2007; Osayemwenre and Meyer, 2014), also EVA and aluminum film backsheet has been reported in the literature (Myong et al., 2014). Cells laminated with EVA and Tedlar film or polyolefin (polyisobutylene as the main polymer chain) layer deposited in liquid form survived extensive aging testing, including a 2000 h test at a 2.5 atmospheres pressure, 127 °C temperature and 80% RH (Hayashi et al., 1994). Flexible a-Si cells with polyester and nylon film superstrates with different encapsulants, e.g. EVA, all failed long-term stability experiment (Pern and Glick, 2000). UV-curable hyperbranched polymer and silica nanoparticle composite with a moth-eye pattern as an antireflective coating on the front glass reduced light reflectance of the front glass substrate from 8% to 4% (González Lazo et al., 2015), see Fig. 5.

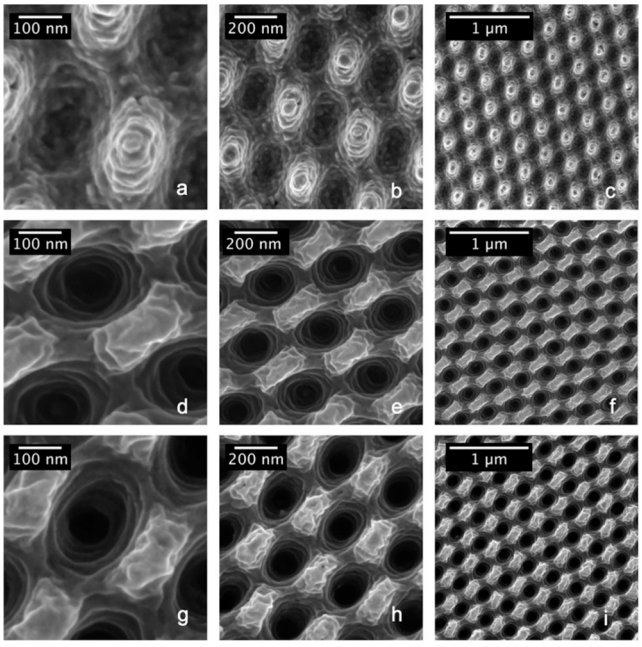

Fig. 5. SEM images of the moth-eye pattern of used as antireflective coating of a-Si cells. a)-c) the nickel master of the structure, d)-f) the structure in a hyperbranched polymer, g)-i) the structure in a hyperbranched polymer-silica composite. Reprinted from (González Lazo et al., 2015).

The main observations from thin film solar cell encapsulation are the following:

- EVA & glass back- and frontsheets are the most used encapsulation materials in thin film solar cells;
- Different multilayer structures containing e.g. polymers are promising alternative encapsulants;
- Added functionalities in encapsulants may improve e.g. the optical properties of the solar cells;
- (Molten) glass matrix contained most of the toxic Cd of CdTE cells in a fire.

5. Encapsulation of emerging solar cells

5.1. Organic solar cell encapsulation

Organic solar cells (OSCs) use small organic molecules and conductive organic polymers for light absorption, charge separation and charge transport. The molecules employed in OSCs are solution-processable and cheap, and the advantages of OSCs are mechanical flexibility and low-cost fabrication (Bazaka et al., 2017a; Nelson, 2011). High PCEs have been demonstrated for OSCs in the recent years. The PCE record of a single junction OSC with the structure of glass/ITO/PEDOT:PSS/PBDB-TF:NFA/PFN-Br/Al reached 17.8% (17.3% certified) (Cui et al., 2020), and a tandem OSC fabricated with the structure of ITO/ZnO/PFN-Br/PBDB-T:FM/M-PEDOT/ZnO/ (PTB7-Th:O6T-4F:$PC_{71}BM$ or PTB7-Th:O6T-4F)/MoO_3/Ag had a 17.4% PCE (17.3% certified) (Meng et al., 2018). The typical OSC materials degrade rapidly when exposed to ambient oxygen and water (Topolniak et al., 2017), and OSCs have only passed accelerated aging tests of several thousand hours so far (Giannouli et al., 2015), which is a key issue preventing their large-scale commercialization. To overcome this problem, a lot of scientific effort has been directed into developing encapsulation techniques of OSCs to reach adequate long-term stabilities (Lee et al., 2013). Effective and cheap encapsulation of OSCs is one of the best ways to prevent moisture and oxygen ingress into the devices and to achieve a long lifetime and also successful commercialization (Uddin et al., 2019).

Rigid encapsulation strategies, such as encapsulating an OSC prepared on a glass superstrate with a frame shaped thermosetting epoxy sealant and an aluminum backplate, have been demonstrated (Krebs, 2006), but because flexibility is an important parameter for commercial OSC applications (Juillard et al., 2018), different flexible encapsulation structures have also been demonstrated, such as single layer (e.g. EVA, inorganic materials) and multilayer thin film encapsulants (Ahmad et al., 2013). Channa et al. employed a perhydropolysilazane / acrylic adhesive multilayer structure as the the OSC encapsulant, and the cell retained 71% of its initial PCE in an ambient light soaking test (Channa et al., 2019). Cros et al. suggested that a barrier material with a WVTR of 10^{-3} $gm^{-2}day^{-1}$ is sufficient to protect OSCs against atmospheric agents for several thousand hours in an accelerated aging test, corresponding to several years in real life outdoor conditions (Cros et al., 2011). They proposed a multilayer encapsulant with the structure of polypropylene/polyvinyl alcohol/inorganic layer/polyethylene, that had a WVTR of $9x10^{-3}$ $gm^{-2}day^{-1}$. After 4 months of aging (at 38 °C, 100% RH and under continuous illumination of 100 mW/cm^2), the structure maintained the criterion, i.e. a total of 1 g m^{-2} of water had diffused across the encapsulant structure, although the studied cells' PCE had dropped to 50% of the original PCE, in the relatively harsh conditions of the aging test. Kovrov et al. showed that commercial and novel acrylic monomers combined with polymeric additives had a high adhesion to a SiOx-PET back encapsulant sheet, and good compatibility with the OSC active layers, as well as good barried properties (Kovrov et al., 2020). The cells retained 60% of their PCE in a 1200 h light soaking test. Lee et al

demonstrated a UV curable epoxy encapsulation on OSCs with an additional ZnO buffer layer, with which the OSCs suffered a 20.5% drop in their PCEs in a 636 h ambient storage experiment (Lee et al., 2013).

Different evaporation methods are commonly empoloyed in manufacturing thin film encapsulant layers onto OSCs. Jeong et al. realized a washable textile-based OSC, that was encapsulated with a polymer capped alternating Al_2O_3/ZnO multilayer structure deposited by ALD, and achieved a stability of over 30 days, with periodic washing (20 × 10 min washing cycles) of the cells (Jeong et al., 2019). Li et al. reported that un-encapsulated OSCs degraded rapidly when exposed to ambient air, but there was no PCE loss even after 3600 h in an ambient storage test, when the OSCs were encapsulated with a thin film manufactured from hexamethyldisiloxane and oxygen by plasma-enhanced chemical vapor deposition (PECVD) (Li et al., 2013). The resulting encapsulant film had high optical transmission of > 90% in the visible light region, and a low WVTR of $3.6 \times 10^{-6} gm^{-2} day^{-1}$. γ-terpinene was also deposited by PECVD and it improved the cells' storage stability (Bazaka et al., 2017b). Chen et al. encapsulated OSCs with a bilayer of poly(divinylbenzene) (PDVB) and cerium (IV) oxide by initiated chemical vapor deposition (Chen et al., 2015). The solar cells were subjected to a dark storage test at 40 °C in ambient air, in which the un-encapsulated OSCs showed an average half-life of 20 h and the encapsulated OSCs a 5-fold improved half-life.

The main observations from OSC encapsulation are the following:

- The materials and methods of OSC encapsulation may be compatible with PSCs, since the cell types may e.g. utilize same contact materials;
- It is possible to create washable OSCs with an inorganic multilayer structure encapsulant;
- Very low WVTR of $3.6 \times 10^{-6} gm^{-2} day^{-1}$ can be achieved with a hybrid organic–inorganic single layer deposited by CVD.

5.2. Dye-sensitized solar cell encapsulation

Dye-sensitized solar cells (DSSCs) have experienced substantial performance and long-term stability improvements since the first publication by O'Regan and Grätzel in 1991 (O'Regan and Grätzel, 1991). The advantages of DSSCs include low-cost of starting materials and easy manufacturing methods, that could be upscaled to large-scale industrial roll-to-roll deposition processes (e.g. screen printing, inkjet printing) (Hashmi et al., 2016; Jung et al., 2018; Mariani et al., 2015), good performance in low intensity light conditions (Freitag et al., 2017), possibility to produce flexible and light-weight devices, and versatility regarding the color and transparency (Hagfeldt et al., 2010; Huaulmé et al., 2020). On the other hand, a possible disadvantage of DSSCs is that the most efficient devices to date are based on liquid electrolytes (Kakiage et al., 2015; Mathew et al., 2014), that cause unique stability issues for the cells (Asghar et al., 2010) and make their encapsulation an important and challenging task (Boschloo, 2019; Desilvestro et al., 2010). To overcome the liquid electrolyte-related issues, many studies have been conducted to develop solid-state (Benesperi et al., 2018) and quasi-solid-state DSSCs (Federico Bella et al., 2016; Yun et al., 2016), although the stability of solid-state DSSCs depends also on adequate encapsulation.

The main types of DSCC edge sealing and encapsulation materials include thermoplastic polymers (Duan et al., 2015; Wang et al., 2006), elastomeric polymers (Kang et al., 2015; Yuwawech et al., 2018, 2017), UV-curable adhesives (Cao et al., 2018; Chiang et al., 2015; Kawata et al., 2015), and glass frits (Ivanou et al., 2016; Lee et al., 2011; Ribeiro et al., 2012; Sastrawan et al., 2006a). Thermoplastic polymers such as Surlyn® and Bynel® (Dow Inc.) are the most widely used materials to seal laboratory scale DSSCs (Desilvestro et al., 2010; Sharma et al., 2018). Surlyn® 1702 is an ethylene and methacrylate acid copolymer with a melting point of 93 °C, and Bynel® 4164 is a low-density polyethylene maleic anhydride-modified resin with a melting point of 127 °C (Dow Chemical Company, 2019a, 2019b; Visco et al., 2019). One issue related to the thermoplastic edge sealants is their relatively high WVTR values. For instance, a 50 μm thick Bynel foil has a 1 g m^{-2} d^{-1} WVTR (De Rossi et al., 2016), while Surlyn exhibits an around 11 g m^{-2} d^{-1} WVTR (Lertngim et al., 2017), which can also contribute to the degradation of devices (De Rossi et al., 2016). Fig. 6 shows a schematic image of a DSSC sealed with thermoplastic polymer.

Advantages of the thermoplastic polymer sealants are their functionality (i.e. to act both as the sealant and the spacer, and the encapsulant), compatibility with roll-to-roll deposition techniques and transparency. However, the heating required when sealing the devices with the thermoplastic polymers may cause undesired effects, such as dye desorption (Jo et al., 2012), solvent evaporation (Sommeling et al., 2004), and degradation of the electrolyte components (Asghar et al., 2010; Chiang et al., 2015). In addition, the thermoplastic polymers have limitations related to their thermal stabilities under high temperatures (>80 °C) and their WVTR in high humidity environments, which may affect the long-term stability of the devices (Fakharuddin et al., 2014; Nath et al., 2017; Visco et al., 2019). However, there are only a few studies focusing on the development of novel thermoplastic sealants, such as copolymers or polymer nanocomposites (Lertngim et al., 2017; Nath et al., 2017).

Adhesive UV-curable edge sealants exhibit some attractive advantages, such as possibility for fast and easy room temperature processing, good adhesion to the substrates, and high thermal stability (Cao et al., 2018; Yeoh et al., 2019). Recently, Grätzel et al. demonstrated a DSSC architecture where a PE and a CE were joined directly together and sealed (i.e. the edges and the electrolyte filling holes) with an UV-cured adhesive (ThreeBond) (Cao et al., 2018), omitting the spacer and resulting "direct contact" between the PE and the CE, as shown in Fig. 7. Chiang et al. studied UV-curable adhesives by varying the type and the amount of acrylate monomers, and the amount of a fluorosurfactant as an additive (Chiang et al., 2019). The devices prepared with UV-curable adhesive containing 10 wt% acrylic acid monomer and 3–4 wt% fluorosurfactant additive showed the best performance in a thermal stability test (i.e. 65 °C for around 45 days). The fluorosurfactant improves the encapsulant electrolyte corrosion resistance but it can also reduce the adhesion strength of the adhesives and the performance of devices when present in excess.

Glass-frit is an interesting DSSC encapsulation method (Hinsch et al., 2008), that consists of a glass-based paste that is applied on the substrate edges by screen printing, followed by a bonding process that is carried out by thermo-compression or with a laser (Ivanou et al., 2016; Knechtel, 2005; Sastrawan et al., 2006a). This encapsulation method presents superior thermal and chemical stability, in addition to chemical inertness toward both the electrolyte and the metal contacts (Sastrawan et al., 2006a). However, the main disadvantage of the method is the high

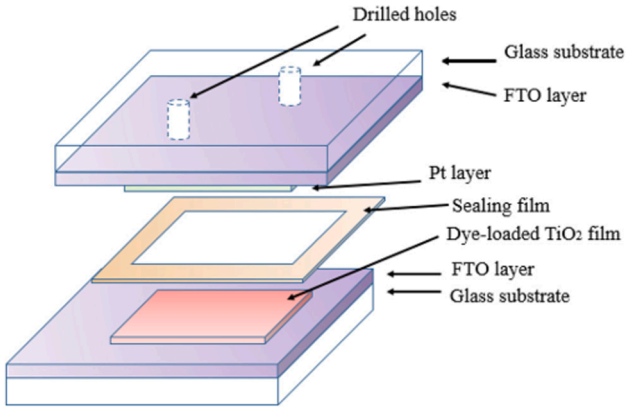

Fig. 6. Illustration of a DSSC sealed with a frame-shaped thermoplastic polymer spacer, reprinted from (Yeoh et al., 2019).

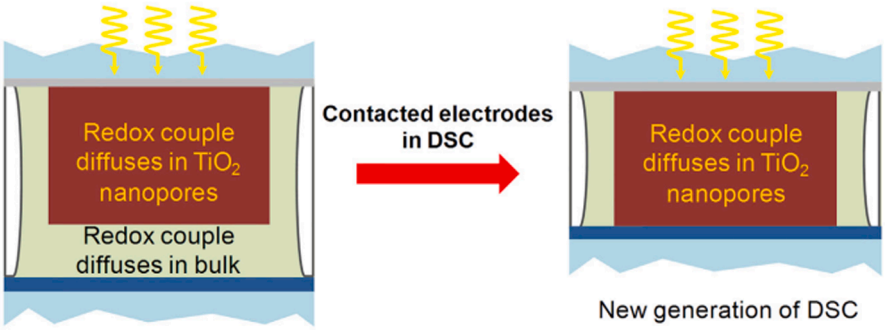

Fig. 7. A traditional DSSC device using a spacer sealant (left) and a DSSC architecture employing direct contact of PE and CE (right) with UV-curable edge sealant. Reprinted from (Cao et al., 2018).

processing temperature, that is over 580 °C for the thermo-compression method and around 330 °C for the laser-assisted method (Ivanou et al., 2016; Ribeiro et al., 2012; Sastrawan et al., 2006b). Therefore special cell manufacturing processes are required for the other device components, and the method is not applicable with flexible substrates (Baxter, 2012; Desilvestro et al., 2010).

Flexible polymer DSSC substrates are permeable, with high WVTR values (i.e. 3.9–17 g m^{-2} d^{-1}), meaning that extra encapsulation needs to be utilized in flexible DSSCs, e.g. a transparent ultrahigh barrier film, UHB (De Rossi et al., 2016) or cellulose-based nanocomposite films (Yang et al., 2016; Yuwawech et al., 2017). An example of an UHB film used in encapsulating a flexible DSSC is the Fraunhofer POLO® multilayer film, which consist of a hybrid inorganic–organic ORMOCER® polymer layer sandwiched between two layers of sputtered zinc-tin-oxide (multilayer WVTR $< 8 \times 10^{-5}$ g m^{-2} d^{-1}) (De Rossi et al., 2016; Fahlteich et al., 2013). The UHB film was attached on top of an ITO-PET-based CE and its use resulted in lifetime improvement of the flexible DSSCs (De Rossi et al., 2016). Another possibility is to encapsulate an entire DSSC with a polymer nanocomposite consisting of polyurethane and cellulose nanocrystals (Yuwawech et al., 2017), that also improved the lifetime of DSSCs.

For flexible DSSCs, an interesting alternative encapsulation strategy is preparing the PE into a groove on a titanium foil, inserting the electrolyte in the groove too, and attaching a transparent ITO-PEN CE substrate with a thermoplastic polymer edge sealant to the Ti foil, as shown in Fig. 8 (Duan et al., 2015; Wang et al., 2015). In this encapsulation scheme, the electrolyte filling holes can be eliminated, and the thermoplastic polymer is used to only edge seal the device. Another method to avoid electrolyte filling holes is to use a thin cellulose aerogel film that absorbs the electrolyte and retains it in its place, while using the edge sealing method (Miettunen et al., 2014; Poskela et al., 2019).

As an example of the elastomeric polymer-type sealant, silicone-based sealants present excellent chemical stability and can be used as the "main" sealant and encapsulant (i.e. as the edge and electrolyte filling hole sealant) or as complementary encapsulation (i.e. on the entire device). As the sealant, this type of polymer provides insufficient protection against moisture ingress due to its porosity, but this can be overcome by a second barrier of protection (e.g. by applying epoxy adhesives) (Baxter, 2012; Desilvestro et al., 2010). However, as the complementary encapsulation, their advantage is resistance against discoloration caused by UV light, in contrast to that of epoxy materials (Kang et al., 2015), that are susceptible to UV degradation (Nikafshar et al., 2017). The physical properties of elastomeric polymers can be improved by preparing e.g. nanocomposites based on polyurethane and cellulose nanocrystals (Yuwawech et al., 2018, 2017).

5.2.1. *UV protection*

The DSSC long-term stability is not only dependent on effective sealing and encapsulation, but also on external agents such as UV light exposure, that may lead to undesirable photoelectrochemical reactions

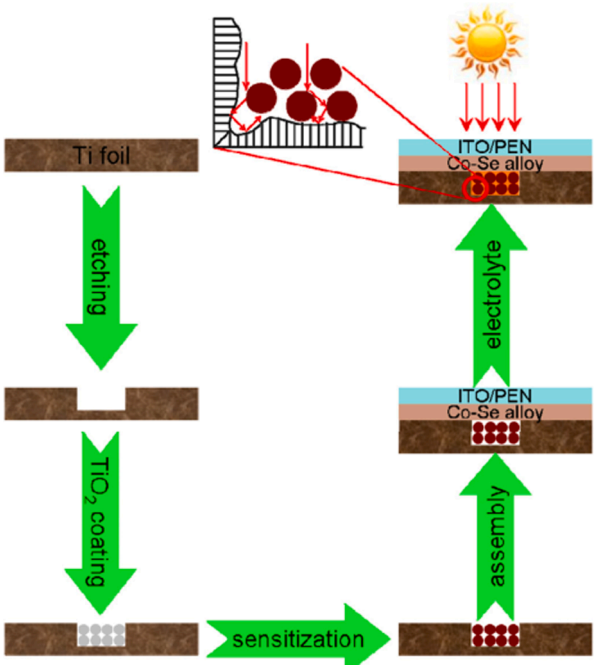

Fig. 8. Illustration of flexible DSSC groove electrolyte filling sealed with thermoplastic polymer. Reprinted from Ref (Duan et al., 2015).

in the cells, causing degradation of the dye or the electrolyte components (Hinsch et al., 2001). For instance exposure to UV light can lead to direct electronic excitation in the TiO_2 layer (Son and Seo, 2020). The electron and hole created in the photoexcitation process enables oxidation and reduction reactions on the TiO_2 surface, that may cause degradation of device components (Asghar et al., 2010; Carnie et al., 2012b; Nakajima and Katoh, 2015). For instance, an organic electrolyte solvent or trace amounts of water in it can react with the UV-generated hole (Nakajima and Katoh, 2015). On the other hand, the electrons in the TiO_2 can react with the I_3^- ion of the electrolyte and form I^- ions (Nakajima and Katoh, 2015). This causes "bleaching" of the I^-/I_3^- redox mediator, when devices are exposed to UV light (Mastroianni et al., 2014), in which the electrolyte changes color from dark yellow to colorless, due to the reduction of the amount of I_3^- ion (Mastroianni et al., 2014; Nakajima and Katoh, 2015).

The direct excitation of the TiO_2 can be prevented by applying a UV cut-off filter on the front side of the cells (Carnie et al., 2012a, 2012b; Son and Seo, 2020). In a recent long-term stability study, light soaking with only visible light was compared to light soaking with the full solar spectrum light with a high quality UV filter (cut-off wavelength 400 nm) (Poskela et al., 2020). The devices protected by the UV filter aged with

full solar spectrum presented faster degradation than the devices aged only with visible light. This implies that either the cut-off wavelength needs to be extended to high energy visible light or that even marginal amounts of UV light are highly detrimental for DSSC (Poskela et al., 2020).

Additionally, polymeric substrates may be directly affected when exposed to UV light. For instance, the optical transmittance of a PEN polymer film is altered under UV light, which means that those substrates require a UV protective barrier (Brown et al., 2014).

The main observations from DSC encapsulation are the following:

- Surlyn and Bynel have relatively high WVTRs and are as such unsuitable for reaching long term stability for DSCs;
- Glass frit is a promising but high-temperature encapsulation method;
- DSC can be manufactured in an etching groove of a Ti metal foil and encapsulated only from one side;
- Photocatalytic TiO_2 causes unique UV light-related stability issues that are not known well yet and whose effects are difficult to counter, and this might have impications on other technologies too, such as PSCs.

5.3. Perovskite solar cell encapsulation

Typically, laboratory scale PSCs are not encapsulated, but the perovskite light absorber layer is sandwiched between other active and passive layers, such as the TiO_2 film on the FTO glass substrate and the Spiro-OMeTAD layer, that protect the perovskite layer somewhat from e.g. atmospheric elements. Several actual encapsulation methods have however been reported, spanning from the early days of perovskite research to the more sophisticated methods of today, and we review them in this chapter. Representative papers of the encapsulation literature (solar cell components, encapsulation type, and possible stability results) are summarized in Table 2.

The first attempts at encapsulating PSCs begun early on, shortly after the initial perovskite breakthrough that happened in 2012: Leijtens et al. employed a two part epoxy drop-cast on the back electrode and a glass cover slip on both mesoporous TiO_2- and Al_2O_3-based PSCs with $MAPbI_{3-x}Cl_x$ absorber, and found out that the alumina-based cells were considerably more stable than the titania counterparts under Xenon lamp light soaking, that entails the UV light component (Leijtens et al., 2013). Burschka et al. sealed sequentially deposited $MAPbI_3$ cells with 50 μm thick "hot-melting polymer" and microscope glass cover slip in argon atmosphere and subjected the cells to a 1000 h MPP tracking experiment under white LED light soaking and 45 °C, and the cells maintained 80% of their PCEs at the 500 h mark (Burschka et al., 2013).

Glass-glass encapsulation with and without additional epoxy or polymeric encapsulation material and varying edge sealants is the most suggested PSC encapsulation method (Cheacharoen et al., 2018b, 2018a; Dong et al., 2016; Dunfield et al., 2018; Dunlap-Shohl et al., 2019; Emami et al., 2019; Jošt et al., 2020; Leijtens et al., 2013; Li et al., 2015; Ma et al., 2020; Matteocci et al., 2016; Ramasamy et al., 2019; Rizzo et al., 2017; Shi et al., 2020, 2017; Stoichkov et al., 2018; Tripathi et al., 2015). Cheacharoen et al. carried out comprehensive work on PSC encapsulation (Cheacharoen et al., 2018b, 2018a), and their "modified" encapsulation method entailed a glass backsheet/ENLIGHT polyolefin encapsulant film and a butyl rubber edge sealant with added desiccant, see Fig. 9. The structure was laminated in a vacuum laminator at a 3000 Pa vacuum, 150 °C temperature and applied mechanical pressing. They employed an ITO glass/NiOx/$Cs_{0.17}FA_{0.83}Pb(Br_{0.17}I_{0.83})_3$/LiF/$C_{60}$/$SnO_2$/ITO/Ag PSC structure, and the chosen encapsulated PSC was stable in thermal cycling and damp-heat stability experiments. Mitzi et al. suggested a lamination process of hot pressing together two "half cells", ITO glass/SnO_2/PCBM/$MAPbI_3$/Spiro-OMeTAD and ITO glass/poly(3,4-ethylene dioxythiophene:polystyrene sulfonate/sorbitol, and found that the process does not affect the cell performance adversely, which can also be considered a glass-glass encapsulation method (Dunlap-Shohl et al., 2019). Recently, low-temperature (65 °C) laser-assisted glass frit encapsulation was demonstrated as a viable PSC encapsulation method. The encapsulation process did not cause notable performance degradation to the perovskite layer and the solar cell performance, and the hermetic sealing proved efficient in humidity and temperature cycling tests (Martins et al., 2020).

Polymer layers are another commonly studied encapsulation material in PSCs. They can be deposited either in liquid form (F Bella et al., 2016; Hwang et al., 2015), as films (Jang et al., 2019; Khadka et al., 2017; B. J. Kim et al., 2019; Weerasinghe et al., 2015), or by evaporation (Idígoras et al., 2018; H. Kim et al., 2019). Parylene-C (poly(p-chloroxylylene)), a common encapsulation material in the electronics industry, was evaporated on $MAPbI_3$-based PSCs and $MAPbI_3$ films, and both the cells and the films withstood exposure to water droplets (H. Kim et al., 2019). Weerasinghe et al. demonstrated a Viewbarrier® film enveloped (front and back encapsulated) flexible PSC that retained full performance in a 500 h dark ambient storage test (Weerasinghe et al., 2015). Also adding just Kapton polyimide tape on the Spiro-OMETAD/Ag layer (B. Li et al., 2018) or copper tape directly on the PCBM electron contact layer (Shao et al., 2015) yielded promising preliminary stability results, meaning these materials could be utilized as facile "laboratory" encapsulants for obtaining improved short-term stabilities for the cells. A multilayer polymer film encapsulation structure was used in a washable flexible PSC that could be used in textile integration; the cells were successfully exposed to multiple crumpling cycles while in a detergent solution without performance decay (Huang et al., 2021), see Fig. 10.

More complex structures and added functionalities, such as UV down-conversing dyes mixed in UV curable fluoropolymer encapsulant layers have also been suggested. Bella et al. obtained very promising results with PSCs with said front and back encapsulants, in detailed UV light soaking, outdoor and a damp-heat testing, at V_{OC}, where cells retained 95–98% of their PCEs (F Bella et al., 2016). A schematic image and scanning electron micrograph of the structure is shown in Fig. 11. ZrO_2 nanoparticles were added in a silane encapsulant to improve its hydrophobicity, and the cells withstood extensive aging studies including MPPT, temperature cycling and water immersion (Luo et al., 2020).

Single- and multilayer thin film layers have been successfully used as the back encapsulant layers in PSCs. Good ambient storage stabilities were obtained with Al_2O_3 single layer (Choi et al., 2018). Wang et al. used molecular layer deposited alucone on ITO/SnO_2/$MAPbI_3$/Spiro-OMeTAD/Ag cells and obtained a very low WVTR for the structure that survived a 2000 h dark test at 30 °C and 80% relative humidity. PSCs encapsulated with a multilayer structure based on ALD-Al_2O_3 and thermally evaporated 1H,1H,2H,2H-perfluorodecyltrichlorosilane retained around 90% of their PCE in a 1000 h light soaking experiment and 80% of PCE in a 1500 h damp-heat aging test (Lv et al., 2020). Also sputtered SiO_2 thin films were demonstrated to protect PSCs from high ambient humidity, sputtering being possibly a more cost-effective thin film deposition technique than ALD (Hosseinian Ahangharnejhad et al., 2021).

Furthermore, different carbon allotropes utilized as the PSC HTM layer can be considered as "additional" encapsulant materials due to their hydrophobic nature, and impressive stabilities have indeed been observed with encapsulated carbon-based monolithic PSCs. Ito et al. kept a glass-glass encapsulated mp-TiO2/$MAPbI_3$/ZrO_2/C PSCs (the back glass attached with UV curing "glue") in a 100 °C oven in the dark for 7000 h and took the cells out only for IV measurements, structure displayed in Fig. 12 (Baranwal et al., 2019). They observed that the cells degraded slowly up to the 4500 h mark retaining 90% of the original PCE, and started to degrade exponentially after that, to 45% of the initial PCE at 7000 h, showing that the commonly discussed MA^+ ion volatility in $MAPbI_3$-based cells is not necessarily an issue with the right choice of other cell components. Others subjected similar cells employing 5-ammoniumvaleric acid iodide-stabilized $MAPbI_3$ encapsulated by a

Table 2
Summary of different PSC encapsulation methods. Spiro refers to Spiro-OMeTAD, VOC to open-circuit voltage, and MPPT to maximum power point tracking.

Author	PSC stack	Encapsulant	Stability experiment	Result
GLASS-GLASS				
Lejtens 2013	FTO/dTiO2/mpAl2O3/MAPbI3-xClx/ Spiro/Au &dTiO2/mpTiO2/MAPbI3-xClx/ Spiro/Au	Two part epoxy drop cast + glass cover	1 sun Xenon lamp, VOC, 40 °C in air, 5 hr for TiO2 cell w UV filter and 1000 hr for Al2O3 cell w/o UV filter	TiO2 cells degrade rapidly, Al2O3 cells: PCE 10 -> 5% at 200 hr mark, stable after that
Burschka 2013	FTO/mpTiO2/MAPbI3/Spiro/Au	50 um "hot-melting polymer" and microscope coverslip	1000 hr MPPT under white LED & 45 °C	PCE drops to 80% at 500 hr mark
Han 2015	FTO/mpTiO2/MAPbI3/Spiro/Ag	A. UV curable epoxy + glass B. UV epoxy edge sealant + desiccant film + glass	1 sun metal halide lamp, VOC, different temperatures and humidities for ~ 100 hr	cells degrade considerably in all conditions, method B more stable
Li 2015	FTO/mpTiO2/(5-AVA)xMA1-xPbI3/ZrO2/ C	Thin glass piece+Surlyn frame spacer+unnamed epoxy resin sealant	A. 7 day outdoor test at VOC in Jeddah, Saudi-Arabia B. 44 day MPPT in 1 sun white LED light and Ar (unsealed devices) C. 3 months 85 °C test in an oven at VOC	A. PCE stable B. Stable C. Few percent drop in PCE
Dong 2016	FTO/planar TiO2/MAPbI3/Spiro/MoO3/ Al	A. 1 mm glass only B. 1 mm glass + desiccant film C. SiO2+desiccant+glass D. Graphene oxide+desicc.+glass; UV curable epoxy edge sealant	1 sun (solar simulator) 85 °C/ 65%RH for 48 hr	C. PCE drops to 80%, for others to 60%
Matteocci 2016	large area (1.05 cm2) FTO/mpTiO2/ MAPbI3/Spiro/Au	several advanced methods, Kapton+UV curable glue+glass+UV curable glue edge sealant	40-50 °C/85%RH test; 1 sun LED light, MPPT, 250 hr	PCE drops to 80% in damp heat test; PCE 14->10% in MPPT
Shi 2017	FTO/mpTiO2/FAPbI3/PTAA/Au	A. Polyisobutylene (PIB) film edge sealant+glass (on gold) B. Same as B but with Au feedthrough to FTO C. Same as B but PIB encapsulant "everywhere"	A. Damp heat test 85 °C, 85% RH B. thermal cycling −40 to 85 °C	A. And B. Encapsulated cells degrade in damp-heat test C. Encapsulated cells survibe both damp-heat and therm cycling tests
Cheacharoen 2018	ITO/NiOx/Cs0.17FA0.83Pb(Br0.17I0.83) 3/LiF/C60/SnO2/ITO/Ag	several methods, Enlight polyolefin encapsulant + butyl rubber w desiccant edge sealant with cover glass (backsheet) and Ag feedthroughs best, laminated with hot vacuum press	A. Thermal cycling -40 - 85 °C B. Dry heat 25%RH/85 °C/ damp heat 85%/85 °C, dry heat also in N2	Cells survive A. And B. Tests well
Stoichkov 2018	ITO/NiOx/MAPbI3 or Cs0.05 (FA0.83MA0.17)95PbI(0.87Br0.13)3/ PC60BM/BCP/Ag	light curable encapsulant + cover glass + UV curable edge sealant; made into modules with UV filter + glass backplane + epoxy edge sealant	23 day outdoor measurements in North-Wales, cells kept at VOC	All cells degrade linearly to 0% PCE
Emami 2019	"Empty cells" to demonstrate low temp	Laser assisted glass frit sealing at 120 °C	-	proof of concept
Ramasamy 2019	FTO/mpTiO2/MAPbI3/Spiro/Au	A. glass + UV curable epoxy edge sealant B. Surlyn gasket + glass	Dark storage test at 30 °C/50% RH	A. PCE drops to 80% B. PCE drops to 70%
Fu 2019	FTO/mpTiO2/(5-AVA)xMA1-xPbI3/ZrO2/ C	glass + hotmelt (polyolefin/polyurethane/ EVA) laminated at 80-90 °C; PU chosen because no effect on PCE; modules encapsulated with metal frames + silicone	A. 85 °C heating for 325 hr B. Outdoor test with resistor for the modules for 2136 hr	A. No performance degradation B. Module maintains 97.5% of PCE
Dunlap-Shohl 2019	ITO/SnO2/PCBM/MAPbI3/Spiro/D-sorbitol/PEDOT:PSS/ITO	"Half cells" ITO/SnO2/PCBM/MAPbI3/ Spiro and D-sorbitol/PEDOT:PSS/ITO pressed together at 120 °C	-	proof of concept
Baranwal 2019	FTO/mpTiO2/MAPbI3/ZrO2/carbon	UV-curable glue + glass	7000 hours at a 100 °C oven	Cells degrade linearly up to 4500 hr, retain 90% of PCE, degrade exponentially after that, retain 45% of PCE at 7000 hr
Ma 2020	ITO/SnO2/Rb0.09Cs0.05 [(FA0.85MA0.15)Pb(I0.85Br0.15)3]/ Spiro/Au	UV-cured adhesive edge sealant + paraffin encapsulant + glass	A. Steady state PL spectra tracking at constant illumination B. 1 sun LED light, MPPT, 20 °C, 30-50%RH for 1000 hr C. Several damp-heat tests	A. No phase segregation B. Retains 80% of PCE C. Retains PCE quite well
Jošt 2020	ITO/MeO-2PACz/Cs0.05(FA0.83MA0.17) Pb1.1(I0.83Br0.17)3/C60/SnO2/Cu	two componet resin edge sealant + glass & "cells put in a closed sealed plastic box with glass cover"	Outdoor rooftop MPPT at University of Ljubljana for ~3 months	"performance ratio" (calculated energy yield) drops to around 20%
Shi 2020	FTO/mpTiO2/Cs0.05FA0.8MA0.15Pb (I0.85 Br0.15)3 or FA0.85MA0.15Pb (I0.85Br0.15)3/PTAA/Au	A. PIB blanket encapsulation + glass B. PIB edge sealant + glass C. PO blanket encapsulation + glass	A. Damp-heat 85 °C/85% RH B. Humidity-freeze -40 - 85 °C/ 85% RH	A. Damp-heat: CsFAMA with PIB blanket passes, others fail B. Humidity-freeze: CsFA and CsFAMA pass with PIB and PO blanket encaps
Martins 2020	FTO/mpTiO2/Cs0.05(FA0.83MA0.17) Pb1.1(I0.83Br0.17)3/PTAA/Au	modified laser-assisted low-temperature (65C) glass frit	A. 25°C/85%RH for 500 hr B. 50 thermal cycles from -40 to 85 °C	A. Cells are stable B. PCE decreases by 15%
Chen 2021	FTO/mpTiO2/ FA0.80MA0.15Cs0.05PbI2.55Br0.45/ Spiro/Au integrated in a water splitting cell	PIB + glass laminated with vacuum press at 50C & the whole back side coated with acrylic adhesive	immersed in water in water splitting experiments for 13 hr	Cells stable
DEPOSITED POLYMER				

(*continued on next page*)

Table 2 (*continued*)

Author	PSC stack	Encapsulant	Stability experiment	Result
Hwang 2015	FTO/mpTiO2/MAPbI3/Spiro/Au	spin coated commercial Teflon precursor, drying at 70 °C for 30 min	ambient storage test	95% of PCE retained
Bella 2016	FTO/mpTiO2/(FAPbI3)0.85(MAPbBr3)0.15/Spiro/Au	chloro-trifluoro-ethylene vinyl ether resin mixed with a difunctional methacrylic perfluoropolyether oligomer (98:2 weight ratio) w and w/o UV downconversing dye, front and front&back	A. 5 mW/cm2 UV test in Ar for 3 months; in air with 50% RH for additional 3 months B. Outdoor test at 1 sun & VOC at Politecnico di Torino, Italy, for 3 months C. 105 °C/95%RH test for 1 month	A. Front/back coated cells retain 98% (front coated degrade after air & humidity exposition) B. Front/back coated retain 95% PCE C. Front/back coated cells retain 96% of PCE
McKenna 2017	MAPbI3xClx on microscope glass	poly(methylmethacrylate), ethyl cellulose, polycarbonate or poly(4-methyl-1-pentene)) spin coated on the back	ambient thermal test at 60, 80 and 100 °C at 50-70% RH, optical characterization	PMMA outperforms other polymers although all PSC films degrade
Idígoras 2018	FTO/mpTiO2/MaPbI3/Spiro/Au	200 nm adamantande polymer by remote plasma vacuum deposition	A. ambient 85% RH humidity test in the dark B. water immersion	A. Retains 70% PCE in 24 hr B. 5% drop in PCE
Kim 2019	FTO/mpTiO2/MAPbI3/Spiro/Au	Parylene-C (poly(p-chloro xylylene) by evaporation	A. ambient storage test for 196 hr B. Water droplet application	A. No change in PCE B. Retains PCE for 30 min
Jang 2019	FTO/mpTiO2/(FAPbI3)0.85(MAPbBr3)0.15/Spiro/Au	poly(vinyl alcohol-co-ethylene) film with SiO2 and graphene oxide additives attahed with Norland optical adhesive	water dropped on PSC kept on a hot plate at 25 °C	Retains 60% of PCE for 10 hours
Bonomo 2020	ITO/SnO2/Cs0.05(FA0.83MA0.17)Pb(I0.83Br0.17)3/Spiro/Au	drop-cast thermosetting polyurethane	A. ambient storage for 2500 hr B. 1 sun MPPT for 3000 min	A. Cells are stable B. PCE drops from 16% to 12%
THIN-FILM				
Choi 2018	FTO/mpTiO2/(FAPbI3)0.85(MAPbBr3)0.15/Spiro or PTAA/Au	50 nm Al2O3 by ALD	A. Ambient i.e. 25 °C/50%RH for 7500 hr B. 65 °C in N2 for 350 hr C. Damp-heat 65 °C/85%RH for 350 hr	A. 4% PCE frop for PTAA cells, 8% for Spiro B & C. cells degrade, PTAA less than Spiro for both experiments
Lv 2018	ITO/NiOx/MAPbI3/PC61BM/ALD-TiO2/Ag	A. 60 nm Al2O3 by ALD B. 60 nm "stacked" ALD layer with 20 nm intermediate layer with extra (ALD) reaction intermediates	A. 1000 hr dark storage B. 2 hr water immersion (for B cells)	A. A. Cells PCE drops to 60% B. Cells retain 93% of PCE B. B cells retain 95% PCE
Wang 2020	ITO/SnO2/MAPbI3/Spiro/Ag	alucone deposited by molecular layer deposition & plasma enhanced ALD Al203 at 50 °C (two bilayers)	A. 300 min water immersion B. 2000 hr 30 °C & 80% RH	A. Retain 95% of PCE B. Retain 96% of PCE; 1.3x10-5 gm-2day-1 WVTR
Lv 2020	ITO/NiO/MAPbI3/PCBM/Ag	Al2O3/1H,1H,2H,2H-perfluor-odecyltrichlorosilane x 2 double layer	A. 1000 hr 1 sun light soaking B. 1000 hr 60 °C heating C. 1500 hr damp-heat 85 °C/85% RH D. Water immersion	A. & B. Cells retain 90% of PCE C. Retain around 80% of PCE D. Cells stable
Ahangharnejhad 2021	FTO/SnO2/(MAPbI3) or (Cs0.05(FA0.85MA0.15)0.95Pb(I0.85Br0.15)3)/Spiro/Au	RF-sputtered SiO2	A. Ambient storage test for 2 months for single cation cells B. Laser-beam induced current measurement, devices in flowing N2 with 85% RH at 25 °C for both types of cells	A. Single cation devices stable B. Triple cation cells less stable than single cation cells with 45 nm thick SiO2, triple cation becomes more stable with 300 nm SiO2
FREE-STANDING FILM/ADHESIVE				
Weerasinghe 2015	flexible IZO-PET/TiO2/CH3NH3PbI3/Spiro/Au)	467 MP 3M™ Adhesive Transfer Tape & Viewbarrier® film, laminated with an "office laminator" at 100 C A. Covering front and back B. Covering edges too	Ambient storage for ~500 hr	A. Cells degrage B. Cells are stable
Kim 2019	FTO/mpTiO2/(FAPbI3)0.85(MAPbBr3)0.15/Spiro/Au	Norland optical adhesive (NOA)/ polyethylene terephthalate/NOA triple layer back encapsulant + micropatterned NOA front encapsulant	water reservoir in direct contact with the back encapsulant at 25 °C for 540 hr	No degradation
Khadka 2017	ITO/PEDOT:PSS/MAPbI3-xClx/PCBM/TBAI/Ag; TBAI=tetrabutylammonium iodide	transparent plastic well fitted to device size glued with a UV curable resin (UV RESIN XNR5516Z, Nagase ChemeteX Japan)	IV & capacitance measurements (defect states) in ambient for 150 days	PCE drops, deteriotation of interfacial layers coupled with trap assisted recombination
Jang 2019	FTO/mpTiO2/(FAPbI3)0.85(MAPbBr3)0.15/Spiro/Au	poly(vinyl alcohol-co-ethylene) film with SiO2 and graphene oxide additives attahed with Norland optical adhesive	water dropped on PSC kept on a hot plate at 25 °C	Retains 60% of PCE for 10 hours
Shao 2015	ITO/PEDOT:PSS/MAPbI3/PC61BM/Cu tape	commercial Cu tape	Ambient storage for 250 hr	PCE drops from 12.3 to 11%
Li 2018	FTO/SnO2 or mpTiO2/MAPbI(3-x)Brx/Spiro/Ag	2 layers of Kapton (polyimide) tape	A. 1800 s water immersion B. spectroscopies of encapsulated perovskite films in different conditions	A. TiO2 cells retain 89.3% and SnO2 96.3% of PCE B. Encapsulated films more stable than unencapsulated
Huang 2021	PET/EVA/ITO-PET/ NiOx/MAPbI3/EVA/PCBM/PEI/ITO-PET/EVA/PET	PET/EVA/PET-ITO/ NiOx/Perovskite/EVA and PET/EVA/PET-ITO/PEI/PCBM half cells pressed together at 120C	A. 10000 hr storage test at 80% RH B. Detergent soak for 240 min C. 30 crumpling cycles in water	A. PCE drops by 8% B. PCE drops by 5% C. Retains 85% of PCE
COMPOSITE				
Luo 2020	FTO/mpTiO2/(5-AVA)xMA1-xPbI3/ZrO2/C	A. ZrO2 nanoparticles in ethylcellulose and terpineol added in 1H,1H,2H,2H-	A. Indoor storage test at 45% RH for 400 days B. Outdoor	A. A cells stable, B cells PCE decreased 70% B. A cells

(*continued on next page*)

Table 2 (*continued*)

Author	PSC stack	Encapsulant	Stability experiment	Result
		perfluorootyltriethoxysilane, airbrushed on the C electrode, heated 10 min at 120C B. Ossila UV curable encapsulation epoxy with cover glass on C electrode	storage test in transparent box for 150 days C. Indoor 1 sun (with UV) MPPT for 240hr D. Water immersion E. Heating-cooling cycle 85 °C for 4hr, room temperature for 4hr, 100 cycles	stable, B. Cells drops to 50% at 100 days C. A cells stable, B cells PCE decreased 52% D. A cells stable, B cells degrade E. A cells stable, B cells degrade after 40 cycles
Kim J 2020	FTO/SnO2/MAPbI3-xBrx/Spiro/Au	dip coated UV cured PDMS with 0.5 wt% quantum dots + spin coated UV cured perhydropolysilazane	25 °C, 95%RH for 220 hr	Cells retain 90% of PCE

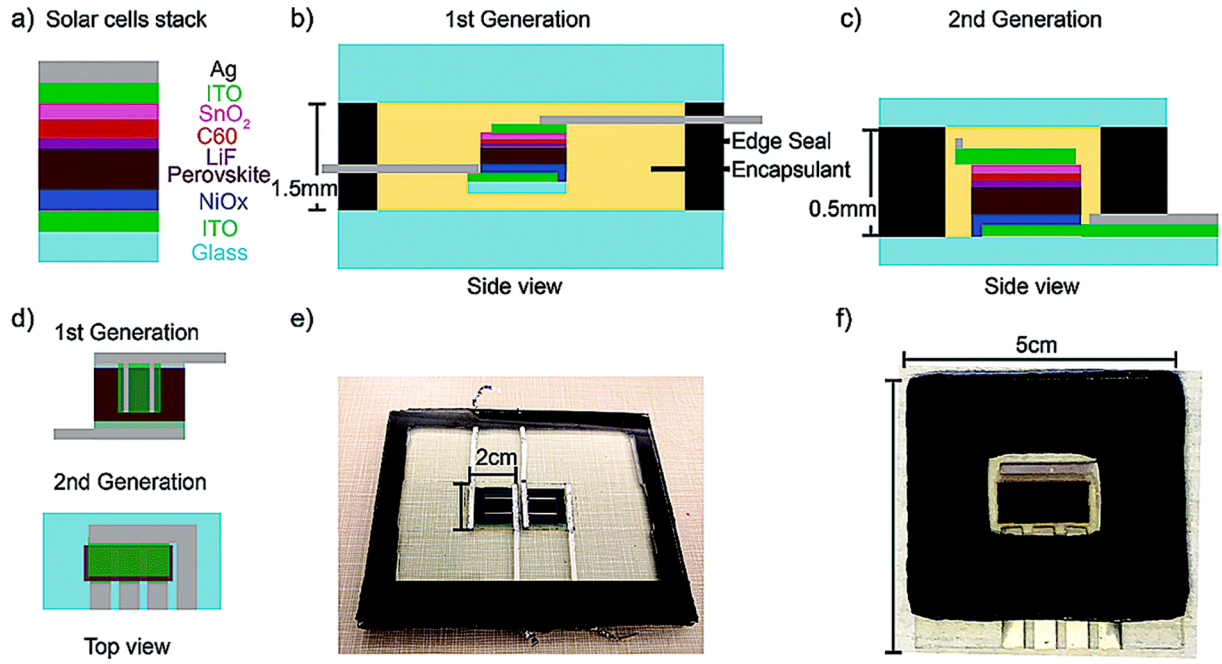

Fig. 9. A PSC encapsulation scheme suggested by Cheacharoen et al. a) the PSC stack used in the study, b) the 1st generation encasulation scheme where the cells are enveloped in two sheets of EVA encapsulant and glass c) the 2nd generation encapsulation scheme where the ITO substrate functions as the front encapsulant and a polyolefin film and glass as the back encapsulants; also there is an electric feedthrough for back contact, d) schematic topview of the two types of encapsulation schemes, e) photograph of the 1st generation scheme, and f) photograph of the 2nd generation scheme. Reprinted from Ref (Cheacharoen et al., 2018a).

glass backsheet and Surlyn edge sealant to an outdoor light soaking tests at MPP and observed little degradation in the performance (Li et al., 2015). Habisreutinger et al. used a single-walled carbon nanotubes: P_3HT:polymethyl methacrylate composite as the hole transporting material (under the Ag contact) in un-encapsulated cells and observed an improved thermal stability in ambient conditions compared to the standard PSCs (Habisreutinger et al., 2014b). It can be concluded that in carbon-contacted PSCs great stabilities meet great commercialization potential, although their PCEs have so far fallen behind those with the standard contact materials.

Lead leakage is a critical environmental and human health-related issue that a PSC encapsulant must address. Jiang et al. used a self-healing epoxy resin with 1-mm-thick glass superstrate as the PSC front encapsulant to contain the lead in the perovskite absorber in case of a glass breakage situation: the resin self-heals at temperatures achieved with solar heat incident on the cells and yielded 375-fold reduction in lead leakage compared to more standard glass-based encapsulation methods (Jiang et al., 2019). Also a cation exchange resin deposited on the back contact was demonstrated successfully to prevent lead leakage from broken minimodules, encapsulated with glass and edge sealant, subjected to water immersion and simulated rain (Chen et al., 2020).

Overall, PSC stability seems to depend on the structure of the solar cell. Albrecht et al. used the simple self-assembled molecular layer hole contacts 2PACz and MeO-2PACz on ITO glass with the PSC stack of ITO/2PACz/perovskite/C_{60}/bathocuproine/Cu and obtained, not only an impressive efficiency of 21.1%, but also stability with a simple cover glass and epoxy encapsulation (Al-Ashouri et al., 2019). They subjected the MeO-2PACz-based cells to extensive outdoor testing, where the cells were however not very stable at higher temperatures, attributed to the chosen perovskite absorber instability (Jošt et al., 2020). It should however be mentioned that, out of all the encapsulated PSCs reported in the literature, the MeO-2PACz-based cells and the carbon-based cells developed by Li et al (Li et al., 2015) were the only ones subjected to both sunlight that contains the UV component (i.e. not only to white LED light used often in many other reports) and electrical load (i.e. the cells were kept at the MPP for the duration of the stability experiment). The other encapsulated cells reported in the literature have been kept under either white LED light (with no UV component), V_{OC} or dark conditions, that are not necessarily realistic conditions for an aging test resembling real-world conditions.

It is not very simple to draw conclusions from the varied literature on PSC encapsulation, because not only the encapsulant structures vary greatly, but also the used perovskite formulations and the cell configurations (whether n-i-p, p-i-n, and the choice of the electrical contact materials) and the stability experiments the cells are subjected to, if any. Therefore, we prepared Table 2, that contains the cell configuration, the

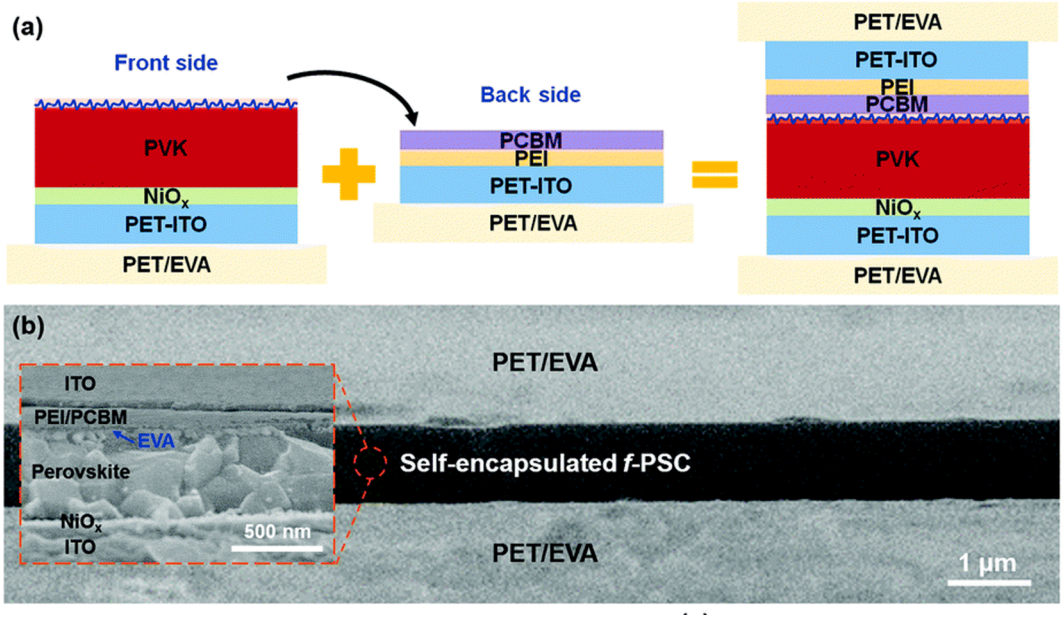

Fig. 10. a) A schematic image of a PET/EVA-encapsulated washable and flexible PSC and its encapsulation method (two "half-cells" attached into an encapsulated PSC), b) a SEM image of the structure.

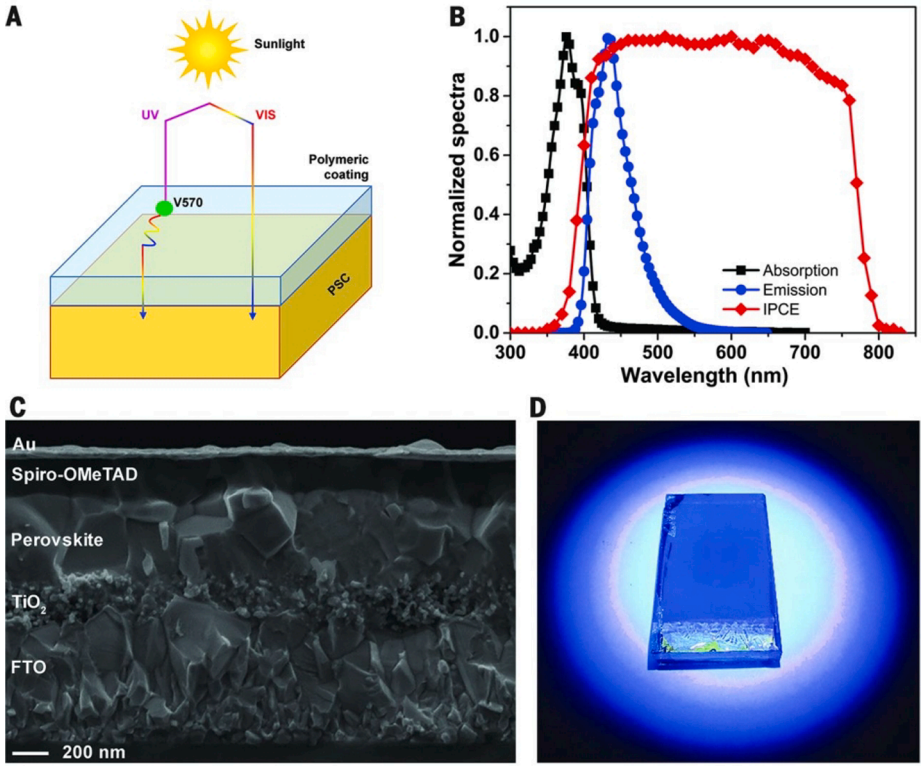

Fig. 11. a) A schematic image of a polymeric encapsulant in which a UV down-conversing dye is embedded, b) Absorption and emission spectra of the UV down-conversing dye and the incident photon to collected electron spectrum of the PSC, c) SEM image and d) a photograph of the PSC. Reprinted from Ref (F Bella et al., 2016).

perovskite formula, the encapsulant type, the stability experiments carried out and the result of the said experiment, which we hope that the reader may use as a "handbook" and choose the encapsulation strategy most suitable for them, the strategies spanning from simple "lab encapsulation methods" to improve the cell "storability" to complex structures that may be subjected to thorough aging experiments. However, as our review shows, several successful encapsulation materials and methods have been demonstrated based both on e.g. rigid glass sheets and different flexible materials, demonstrating that considerable progress has been made on that front recently.

The main observations from PSC encapsulation are the following:

- Thermoplastic polyolefin & glass backsheet and butyl rubber edge sealant is a possible option for PSC encapsulation. The encapsulant

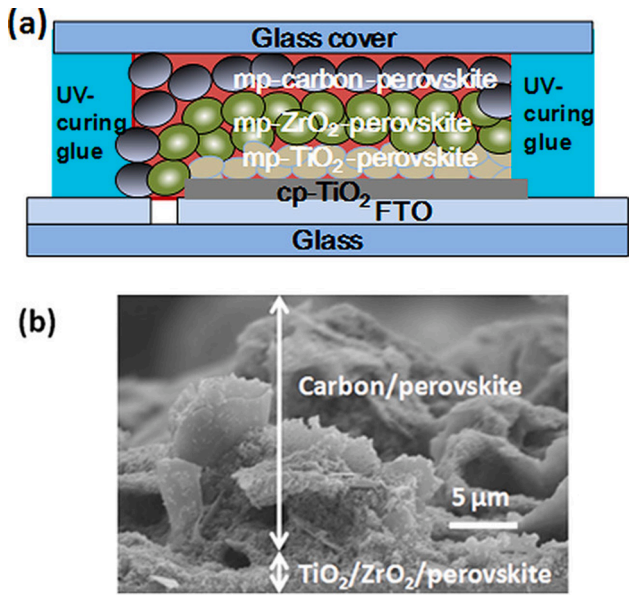

Fig. 12. a) Schematic image of an encapsulated monolithic carbon mesoporous carbon-based PSC, b) electron micrograph of active layers. Reprinted from Ref (Baranwal et al., 2019).

was applied with 150 °C vacuum lamination, and a PSC with certain structure withstood the process without losses in cell performance, however the encapsulation method results in a rigid solar cell;

- Low-temperature glass frit is a viable option for PSC encapsulation;
- PSC water immersion has been successfully demonstrated with several different encapsulation strategies, showing that it is possible to protect PSCs efficiently from water with adequate encapsulation;
- Carbon-based PSCs are among the most stable PSC configurations; carbon's hydrophobicity; offers additional protection and simple encapsulation is sufficient for good stability;
- The field is new, there is several different encapsulation materials and methods, and there are not many highly detailed aging studies carried out on encapsulated PSCs yet.

6. Other aspects of solar cell encapsulation

Next, we briefly discuss additional functionalities and possible future directions of solar cell encapsulation materials and techniques.

A low solar cell PCE can be related not only to issues in the active materials, but also e.g. to reflection, shading, incomplete absorption of light, non-absorption of high wavelength light, and thermalization of short-wavelength light (Day et al., 2019), that can be addressed for instance by additional functionalities in the encapsulant materials. Light management may entail for instance anti-reflection (Jacobs et al., 2019; Wang et al., 2020), scattering (haze) (Li et al., 2020), photon up-conversion (Nguyen et al., 2017), photon down-conversion (Zhao et al., 2019), photon down-shifting (Alexandre et al., 2019) and UV protection functionalities (Hayden et al., 2019; Zhang et al., 2019).

Antireflective coatings and surface structures enhance the absorption of light in the active layer (Kim et al., 2020). Yun et al. produced a silicone-based encapsulation for silicon solar cells combining different 1D patterns in the submicron and micrometer range (hills and valleys, waves, and cylindrical lens structures) and obtained an omnidirectional PCE enhancement of up to 2% (Yun et al., 2020a, 2020b). Another feature that such surface patterning can provide is improvement of moisture and water resistance, combined with self-cleaning properties (Idígoras et al., 2018; Zhi and Zhang, 2018). However, these properties depend on the type of patterning, as Wang et al. observed (Wang et al., 2017). Their work showed that close-packed nanopillar structures imprinted on an ethylene-tetrafluoroethylene copolymer film coating of a triple-junction thin film solar cell presents high hydrophobicity but not good self-cleaning and light-trapping properties. On the other hand, stripe-like triangular prism structures exhibit hydrophobicity, self-cleaning, and light trapping properties and increased the cells' PCE by 5.5%. Surface patterning has however also drawbacks that are related to for instance the challenging manufacturing processes of micro- and nanoscale structures (Ha et al., 2014).

Alternative bio-based materials such as nanocellulose and "transparent wood" (delignified wood filled by a polymer with the same refractive index (Li et al., 2019)) have been proposed to be used in the preparation of anti-reflective coatings (Fang et al., 2015; Ha et al., 2014; Podsiadlo et al., 2007). However, because of the hydroxyl group networks in nanocellulose materials, they interact strongly with ambient water and oxygen (Shen and Gnanakaran, 2009). Therefore their water and oxygen resistance has to be developed further before they can be applied in photovoltaic devices. This could be achieved by the same hydroxyl groups: their high reactivity enables also easy chemical modification and e.g. utilizing cross-linking (Hossain et al., 2020), to improve their barrier properties. On the other hand transparent wood does not have the same hydrophilicity property because it can easily be impregnated with hydrophobic polymer, decreasing its interaction with water and oxygen (Y. Li et al., 2018; Mi et al., 2020).

With bio-based materials, it is also possible to produce a beneficial optical property: haze. Haze is defined as the ratio of transmitted light that is diffusely scattered in the forward direction to the total transmitted light, and it is created by deformations in the material structure, that can be achieved with e.g. use of additional particles, pores, or surface roughness (Jacucci et al., 2020). In general, haze improves a solar cell's performance by improving light absorption (Li et al., 2019). The improvement of light scattering and absorption using nanocellulose films as front layers has already been shown in PSCs (Hou et al., 2020) and in OSCs (Wu et al., 2020).

The effects of harmful light, such as UV light, can be prevented by using composite encapsulation systems. One of the most common methods for UV protection is using semiconductor nanoparticle layers, such as zinc oxide (Aljaiuossi et al., 2019) and TiO_2 (Zhu et al., 2021) layers, as the solar cell front layer. These films block UV-A (ZnO) and UV-B (TiO_2), separately, and together they yield broadband UV protection (Smijs and Pavel, 2011). However, in the search for more sustainable materials, bio-based materials such as lignin nanoparticles, rise as an option for UV protective layers due to the chromophore groups that absorb almost all incident UV light (Sadeghifar and Ragauskas, 2020).

Another group of materials used in UV protection that can also yield PCE enhancement is photoconverters (Day et al., 2019; de la Mora et al., 2017; Khare, 2020; Moffatt et al., 2020; Nonat and Fix, 2019; Rajeswari et al., 2020). These materials function by converting: (i) one incident high-energy photon into two (or more) lower energy photons (down-converters), (ii) two (or more) low-energy photons into one higher energy photon (up-converters), or (iii) one high-energy photon into one lower-energy photon (down-shifters) (Huang et al., 2013). Traditionally these materials are composed of rare-earth-doped crystalline materials (Sun et al., 2021), but the search for alternative, more environmentally friendly options has resulted also in the discovery of novel materials, such as quantum dots and organo-metallic dyes (Day et al., 2019). Carbon quantum dots obtained from bio-based materials have shown promise in light management, because they exhibit properties such as high fluorescence, photo-bleaching resistance, and wavelength-dependent photoluminescence behavior (Alas et al., 2020).

7. Conclusions

In this review article we have explored and discussed encapsulation materials and methods of established and emerging photovoltaic techniques with special focus on PSC encapsulation. The materials and methods range from the established ones used in the crystalline silicon

photovoltaics industry to the experimental ones used in academic research on emerging solar cells. Perovskite solar cells as the newest emerging solar cell technology may take benefit from the lessons-learnt from the present encapsulation materials and methods of all the other solar cell technologies, and novel innovations that benefit the whole solar cell community may be adopted from PSC, as well as other emerging PV technologies. Ethylene vinyl acetate layers combined with glass front and backsheets and a polyisobutylene edge sealant is the dominant encapsulation technology in the PV industry, but several alternative materials have also been proposed. Similar encapsulation scheme is possible for PSCs too: a thermoplastic polyolefin and glass frontsheet encapsulation scheme, combined with butyl rubber edge sealant, attached via vacuum lamination, is a viable technique for PSC use. Alternative PSC encapsulation strategies based on for instance fluoropolymeric composites have yielded promising stability results, and additional functionalities can be combined with encapsulants. Future encapsulation materials could entail encapsulants with added functionalities and biobased starting materials.

Declaration of Competing Interest

The authors declare that they have no known competing financial interests or personal relationships that could have appeared to influence the work reported in this paper.

Acknowledgements

K.A. is grateful for Jane and Aatos Erkko foundation project ASPIRE for funding the study. G.G.S., J.K. and K.M. thank Academy of Finland (projects BioEST and Substainable, and flagship project FinnCERES). X. H. thanks for the scholarship by the Chinese Science Council, No. 201706250038.

References

Adothu, B., Bhatt, P., Chattopadhyay, S., Zele, S., Oderkerk, J., Sagar, H.P., Costa, F.R., Mallick, S., 2019. Newly developed thermoplastic polyolefin encapsulant – a potential candidate for crystalline silicon photovoltaic modules encapsulation. Sol. Energy 194, 581–588. https://doi.org/10.1016/j.solener.2019.11.018.

Ahmad, J., Bazaka, K., Anderson, L.J., White, R.D., Jacob, M.V., 2013. Materials and methods for encapsulation of OPV: a review. Renew. Sustain. Energy Rev. 27, 104–117. https://doi.org/10.1016/j.rser.2013.06.027.

Aitola, K., Domanski, K., Correa-Baena, J., Sveinbjörnsson, K., Saliba, M., Abate, A., Grätzel, M., Kauppinen, E., Johansson, E.M.J., Tress, W., Hagfeldt, A., Boschloo, G., 2017. High temperature-stable perovskite solar cell based on low-cost carbon nanotube hole contact. Adv. Mater. 1–5 https://doi.org/10.1002/ADMA.201606398.

Al-Ashouri, A., Magomedov, A., Roß, M., Jošt, M., Talaikis, M., Chistiakova, G., Bertram, T., Márquez, J.A., Köhnen, E., Kasparavičius, E., Levcenco, S., Gil-Escrig, L., Hages, C.J., Schlatmann, R., Rech, B., Malinauskas, T., Unold, T., Kaufmann, C.A., Korte, L., Niaura, G., Getautis, V., Albrecht, S., 2019. Conformal monolayer contacts with lossless interfaces for perovskite single junction and monolithic tandem solar cells. Energy Environ. Sci. 12, 3356–3369. https://doi.org/10.1039/c9ee02268f.

Alas, M.O., Alkas, F.B., Aktas Sukuroglu, A., Genc Alturk, R., Battal, D., 2020. Fluorescent carbon dots are the new quantum dots: an overview of their potential in emerging technologies and nanosafety. J. Mater. Sci. 55, 15074–15105. https://doi.org/10.1007/s10853-020-05054-y.

Alexandre, M., Chapa, M., Haque, S., Mendes, M.J., Águas, H., Fortunato, E., Martins, R., 2019. Optimum luminescent down-shifting properties for high efficiency and stable perovskite solar cells. ACS Appl. Energy Mater. 2, 2930–2938. https://doi.org/10.1021/acsaem.9b00271.

Aljaiuossi, G., Makableh, Y.F., Al-Fandi, M., 2019. Design and optimization of nanostructured UV-filters for efficient and stable perovskite solar cells. Semicond. Sci. Technol. 34, 125014 https://doi.org/10.1088/1361-6641/ab51a0.

Aristidou, N., Sanchez-Molina, I., Chotchuangchutchaval, T., Brown, M., Martinez, L., Rath, T., Haque, S.A., 2015. The role of oxygen in the degradation of methylammonium lead trihalide perovskite photoactive layers. Angew. Chemie - Int. Ed. 54, 8208–8212. https://doi.org/10.1002/anie.201503153.

Arya, R.R., Carlson, D.E., 2002. Amorphous silicon PV module manufacturing at BP solar. Prog. Photovoltaics Res. Appl. 10, 69–76. https://doi.org/10.1002/pip.418.

Asghar, M.I., Miettunen, K., Halme, J., Vahermaa, P., Toivola, M., Aitola, K., Lund, P., 2010. Review of stability for advanced dye solar cells. Energy Environ. Sci. 3, 418. https://doi.org/10.1039/b922801b.

Babayigit, A., Ethirajan, A., Muller, M., Conings, B., 2016. Toxicity of organometal halide perovskite solar cells. Nat. Mater. 15, 247–251. https://doi.org/10.1038/nmat4572.

Baikie, T., Fang, Y., Kadro, J.M., Schreyer, M., Wei, F., Mhaisalkar, S.G., Graetzel, M., White, T.J., 2013. Synthesis and crystal chemistry of the hybrid perovskite (CH 3NH3)PbI3 for solid-state sensitised solar cell applications. J. Mater. Chem. A 1, 5628–5641. https://doi.org/10.1039/c3ta10518k.

Baranwal, A.K., Kanda, H., Shibayama, N., Masutani, H., Peiris, T.A.N., Kanaya, S., Segawa, H., Miyasaka, T., Ito, S., 2019. Thermal degradation analysis of sealed perovskite solar cell with porous carbon electrode at 100 °C for 7000 h. Energy Technol. 7, 245–252. https://doi.org/10.1002/ente.201800572.

Baxter, J.B., 2012. Commercialization of dye sensitized solar cells: present status and future research needs to improve efficiency, stability, and manufacturing. J. Vac. Sci. Technol. A Vacuum, Surfaces, Film. 30, 020801 https://doi.org/10.1116/1.3676433.

Bazaka, K., Ahmad, J., Oelgemöller, M., Uddin, A., Jacob, M.V., 2017a. Photostability of plasma polymerized γ -terpinene thin films for encapsulation of OPV. Sci. Rep. 7, 45599. https://doi.org/10.1038/srep45599.

Bazaka, K., Ahmad, J., Oelgemöller, M., Uddin, A., Jacob, M.V., 2017b. Photostability of plasma polymerized γ -terpinene thin films for encapsulation of OPV. Nat. Publ. Gr. 1–9 https://doi.org/10.1038/srep45599.

Bella, F., Galliano, S., Gerbaldi, C., Viscardi, G., 2016a. Cobalt-based electrolytes for dye-sensitized solar cells: recent advances towards stable devices. Energies 9, 384. https://doi.org/10.3390/en9050384.

Bella, F., Bella, F., Griffini, G., Saracco, G., Grätzel, M., Hagfeldt, A., Turri, S., Gerbaldi, C., 2016b. Improving efficiency and stability of perovskite solar cells with photocurable fluoropolymers. Science (80-.) 354, 203–206. https://doi.org/10.1126/science.aah4046.

Benesperi, I., Michaels, H., Freitag, M., 2018. The researcher's guide to solid-state dye-sensitized solar cells. J. Mater. Chem. C. https://doi.org/10.1039/c8tc03542c.

Bi, D., El-Zohry, A.M., Hagfeldt, A., Boschloo, G., 2014. Improved morphology control using a modified two-step method for efficient perovskite solar cells. ACS Appl. Mater. Interfaces 6, 18751–18757. https://doi.org/10.1021/am504320h.

Boschloo, G., 2019. Improving the performance of dye-sensitized solar cells. Front. Chem. 7, 1–9. https://doi.org/10.3389/fchem.2019.00077.

Brown, T.M., De Rossi, F., Di Giacomo, F., Mincuzzi, G., Zardetto, V., Reale, A., Di Carlo, A., 2014. Progress in flexible dye solar cell materials, processes and devices. J. Mater. Chem. A 2, 10788–10817. https://doi.org/10.1039/c4ta00902a.

Burschka, J., Pellet, N., Moon, S.J., Humphry-Baker, R., Gao, P., Nazeeruddin, M.K., Grätzel, M., 2013. Sequential deposition as a route to high-performance perovskite-sensitized solar cells. Nature 499, 316–319. https://doi.org/10.1038/nature12340.

Cao, Y., Liu, Y., Zakeeruddin, S.M., Hagfeldt, A., Grätzel, M., 2018. Direct contact of selective charge extraction layers enables high-efficiency molecular photovoltaics. Joule 2, 1108–1117. https://doi.org/10.1016/j.joule.2018.03.017.

Carcia, P.F., McLean, R.S., Hegedus, S., 2010. Encapsulation of Cu(InGa)Se2 solar cell with Al 2O3 thin-film moisture barrier grown by atomic layer deposition. Sol. Energy Mater. Sol. Cells 94, 2375–2378. https://doi.org/10.1016/j.solmat.2010.08.021.

Carnie, M., Bryant, D., Watson, T., Worsley, D., 2012a. Photocatalytic oxidation of triiodide in UVA-exposed dye-sensitized solar cells. Int. J. Photoenergy 2012, 8. https://doi.org/10.1155/2012/524590.

Carnie, M., Watson, T., Worsley, D., 2012b. UV Filtering of dye-sensitized solar cells: the effects of varying the UV cut-off upon cell performance and incident photon-to-electron conversion efficiency. Int. J. Photoenergy 2012, 1–9. https://doi.org/10.1155/2012/506132.

Cattaneo, G., Faes, A., Li, H., Galliano, F., Gragert, M., Yao, Y., Despeisse, M., Ballif, C., 2014. Lamination process and encapsulation materials for glass–glass PV module design. Photovoltaics Int. 1, 1–8.

Channa, I.A., Distler, A., Zaiser, M., Brabec, C.J., Egelhaaf, H.J., 2019. Thin film encapsulation of organic solar cells by direct deposition of polysilazanes from solution. Adv. Energy Mater. 9, 1–10. https://doi.org/10.1002/aenm.201900598.

Cheacharoen, R., Boyd, C.C., Burkhard, G.F., Leijtens, T., Raiford, J.A., Bush, K.A., Bent, S.F., McGehee, M.D., 2018a. Encapsulating perovskite solar cells to withstand damp heat and thermal cycling. Sustain. Energy Fuels 2, 2398–2406. https://doi.org/10.1039/c8se00250a.

Cheacharoen, R., Rolston, N., Harwood, D., Bush, K.A., Dauskardt, R.H., McGehee, M.D., 2018b. Design and understanding of encapsulated perovskite solar cells to withstand temperature cycling. Energy Environ. Sci. 11, 144–150. https://doi.org/10.1039/c7ee02564e.

Chen, N., Kovacik, P., Howden, R.M., Wang, X., Lee, S., Gleason, K.K., 2015. Low Substrate Temperature Encapsulation for Flexible Electrodes and Organic Photovoltaics 1–7. https://doi.org/10.1002/aenm.201401442.

Chen, S., Deng, Y., Gu, H., Xu, S., Wang, S., Yu, Z., Blum, V., Huang, J., 2020. Trapping lead in perovskite solar modules with abundant and low-cost cation-exchange resins. Nat. Energy 5, 1003–1011. https://doi.org/10.1038/s41560-020-00716-2.

Chiang, T.H., Chen, C.H., Liu, C.Y., 2015. Effect of sealing with ultraviolet-curable adhesives on the performance of dye-sensitized solar cells. J. Appl. Polym. Sci. 132, 42015. https://doi.org/10.1002/app.42015.

Chiang, T.H., Chen, C.H., Wei, T.C., 2019. Characterization of UV-curable adhesives containing acrylate monomers and fluorosurfactant and their performance in dye-sensitized solar cells in long-term thermal stability tests. J. Appl. Polym. Sci. 136, 1–10. https://doi.org/10.1002/app.47948.

Choi, E.Y., Kim, J., Lim, S., Han, E., Ho-Baillie, A.W.Y., Park, N., 2018. Enhancing stability for organic-inorganic perovskite solar cells by atomic layer deposited Al2O3 encapsulation. Sol. Energy Mater. Sol. Cells 188, 37–45. https://doi.org/10.1016/j.solmat.2018.08.016.

Conings, B., Drijkoningen, J., Gauquelin, N., Babayigit, A., D'Haen, J., D'Olieslaeger, L., Ethirajan, A., Verbeeck, J., Manca, J., Mosconi, E., Angelis, F.D., Boyen, H.-G., 2015. Intrinsic thermal instability of methylammonium lead trihalide perovskite. Adv. Energy Mater. 5, 1500477. https://doi.org/10.1002/aenm.201500477.

Cros, S., De Bettignies, R., Berson, S., Bailly, S., Maisse, P., Lemaitre, N., Guillerez, S., 2011. Definition of encapsulation barrier requirements: a method applied to organic solar cells. Sol. Energy Mater. Sol. Cells 95, S65–S69. https://doi.org/10.1016/j.solmat.2011.01.035.

Cui, Y., Yao, H., Zhang, J., Xian, K., Zhang, T., Hong, L., Wang, Y., Xu, Y., Ma, K., An, C., He, C., Wei, Z., Gao, F., Hou, J., 2020. Single-junction organic photovoltaic cells with approaching 18% efficiency. Adv. Mater. 32, 1–7. https://doi.org/10.1002/adma.201908205.

Czanderna, A.W., Pern, F.J., 1996. Encapsulation of PV modules using ethylene vinyl acetate copolymer as a pottant: a critical review. Sol. Energy Mater. Sol. Cells 43, 101–181. https://doi.org/10.1016/0927-0248(95)00150-6.

Day, J., Senthilarasu, S., Mallick, T.K., 2019. Improving spectral modification for applications in solar cells: a review. Renew. Energy 132, 186–205. https://doi.org/10.1016/j.renene.2018.07.101.

de la Mora, M.B., Amelines-Sarria, O., Monroy, B.M., Hernández-Pérez, C.D., Lugo, J.E., 2017. Materials for downconversion in solar cells: perspectives and challenges. Sol. Energy Mater. Sol. Cells 165, 59–71. https://doi.org/10.1016/j.solmat.2017.02.016.

De Rossi, F., Mincuzzi, G., Di Giacomo, F., Fahlteich, J., Amberg-Schwab, S., Noller, K., Brown, T.M., 2016. A Systematic investigation of permeation barriers for flexible dye-sensitized solar cells. Energy Technol. 4, 1455–1462. https://doi.org/10.1002/ente.201600244.

Dechthummarong, C., Wiengmoon, B., Chenvidhya, D., Jivacate, C., Kirtikara, K., 2010. Physical deterioration of encapsulation and electrical insulation properties of PV modules after long-term operation in Thailand. Sol. Energy Mater. Sol. Cells 94, 1437–1440. https://doi.org/10.1016/j.solmat.2010.03.038.

Desilvestro, H., Bertoz, M., Tulloch, S., Tulloch, G., 2010. Packaging, scale-up and commercialization of dye solar cells. In: Kalyanasundaram, K. (Ed.), Dye-Sensitized Solar Cells. EPFL Press-CRC, Lausanne, pp. 207–249.

Dietrich, S., Pander, M., Sander, M., Schulze, S.H., Ebert, M., 2010. Mechanical and thermomechanical assessment of encapsulated solar cells by finite-element-simulation. Reliab. Photovolt. Cells, Modul. Components, Syst. III 7773, 77730F. https://doi.org/10.1117/12.860661.

Domanski, K., Correa-Baena, J.-P., Mine, N., Nazeeruddin, M.K., Abate, A., Saliba, M., Tress, W., Hagfeldt, A., Grätzel, M., 2016. Not all that glitters is gold: metal-migration-induced degradation in perovskite solar cells. ACS Nano 10, 6306–6314. https://doi.org/10.1021/acsnano.6b02613.

Dong, Q., Liu, F., Wong, M.K., Tam, H.W., Djurišić, A.B., Ng, A., Surya, C., Chan, W.K., Ng, A.M.C., 2016. Encapsulation of perovskite solar cells for high humidity conditions. ChemSusChem 9, 2597–2603. https://doi.org/10.1002/cssc.201600868.

Dow Chemical Company, 2019a. Dow Packaging & Speciality Plastics Product Data Sheet BYNEL ™ 4164 Adhesive Resin [WWW Document].

Dow Chemical Company, 2019b. Dow Packaging & Speciality Plastics Product Data Sheet SURLYN ™ 8940 Ionomer [WWW Document].

Dualeh, A., Gao, P., Seok, S.I., Nazeeruddin, M.K., Grätzel, M., 2014. Thermal behavior of methylammonium lead-trihalide perovskite photovoltaic light harvesters. Chem. Mater. 26, 6160–6164. https://doi.org/10.1021/cm502468k.

Duan, Y., Tang, Q., Li, R., He, B., Yu, L., 2015. An avenue of sealing liquid electrolyte in flexible dye-sensitized solar cells. J. Power Sources 274, 304–309. https://doi.org/10.1016/j.jpowsour.2014.10.068.

Dunfield, S.P., Moore, D.T., Klein, T.R., Fabian, D.M., Christians, J.A., Dixon, A.G., Dou, B., Ardo, S., Beard, M.C., Shaheen, S.E., Berry, J.J., Van Hest, M.F.A.M., 2018. Curtailing perovskite processing limitations via lamination at the perovskite/perovskite interface. ACS Energy Lett. 3, 1192–1197. https://doi.org/10.1021/acsenergylett.8b00548.

Dunlap-Shohl, W.A., Li, T., Mitzi, D.B., 2019. Interfacial effects during rapid lamination within MAPbI3 thin films and solar cells. ACS Appl. Energy Mater. 2, 5083–5093. https://doi.org/10.1021/acsaem.9b00747.

Emami, S., Martins, J., Madureira, R., Hernandez, D., Bernardo, G., Mendes, J., Mendes, A., 2019. Development of hermetic glass frit encapsulation for perovskite solar cells. J. Phys. D. Appl. Phys. 52 https://doi.org/10.1088/1361-6463/aaf1f4.

Fahlteich, J., Amberg-Schwab, S., Weber, U., Noller, K., Miesbauer, O., Boeffel, C., Schiller, N., 2013. Ultra-high barriers for encapsulation of flexible displays and lighting devices. Dig. Tech. Pap. - SID Int. Symp. 44, 354–357. https://doi.org/10.1002/j.2168-0159.2013.tb06219.x.

Fakharuddin, A., Jose, R., Brown, T.M., Fabregat-Santiago, F., Bisquert, J., 2014. A perspective on the production of dye-sensitized solar modules. Energy Environ. Sci. https://doi.org/10.1039/c4ee01724b.

Fang, Z.-Q., Zhu, H.-L., Li, Y.-Y., Liu, Z., Dai, J.-Q., Preston, C., Garner, S., Cimo, P., Chai, X.-S., Chen, G., Hu, L.-B., 2015. Light management in flexible glass by wood cellulose coating. Sci. Rep. 4, 5842. https://doi.org/10.1038/srep05842.

Freitag, M., Teuscher, J., Saygili, Y., Zhang, X., Giordano, F., Liska, P., Hua, J., Zakeeruddin, S.M., Moser, J.E., Grätzel, M., Hagfeldt, A., 2017. Dye-sensitized solar cells for efficient power generation under ambient lighting. Nat. Photonics 11, 372–378. https://doi.org/10.1038/nphoton.2017.60.

Fthenakis, V., Athias, C., Blumenthal, A., Kulur, A., Magliozzo, J., Ng, D., 2020. Sustainability evaluation of CdTe PV: an update. Renew. Sustain. Energy Rev. 123, 109776 https://doi.org/10.1016/j.rser.2020.109776.

Fthenakis, V.M., Fuhrmann, M., Heiser, J., Lanzirotti, A., Fitts, J., Wang, W., 2005. Emissions and encapsulation of cadmium in CdTe PV modules during fires. Prog. Photovoltaics Res. Appl. 13, 713–723. https://doi.org/10.1002/pip.624.

Gawlińska, K., Drabczyk, K., Starowicz, Z., Sobik, P., Drabczyk, B., Zięba, P., 2018. Determination of eva cross-linking degree after lamination process by extraction and optical transmission measuring. Arch. Metall. Mater. 63, 833–838. https://doi.org/10.24425/122411.

Giannouli, M., Drakonakis, V.M., Savva, A., Eleftheriou, P., Florides, G., Choulis, S.A., 2015. Methods for improving the lifetime performance of organic photovoltaics with low-costing encapsulation. ChemPhysChem. https://doi.org/10.1002/cphc.201402749.

González Lazo, M.A., Schüler, A., Haug, F.J., Ballif, C., Månson, J.A.E., Leterrier, Y., 2015. Superhard, antireflective texturized coatings based on hyperbranched polymer composite hybrids for thin-film solar cell encapsulation. Energy Technol. 3, 366–372. https://doi.org/10.1002/ente.201402141.

Goodrich, A., Hacke, P., Wang, Q., Sopori, B., Margolis, R., James, T.L., Woodhouse, M., 2013. A wafer-based monocrystalline silicon photovoltaics road map: Utilizing known technology improvement opportunities for further reductions in manufacturing costs. Sol. Energy Mater. Sol. Cells 114, 110–135. https://doi.org/10.1016/j.solmat.2013.01.030.

Green, M.A., 2007. Thin-film solar cells: Review of materials, technologies and commercial status. J. Mater. Sci. Mater. Electron. 18, 15–19. https://doi.org/10.1007/s10854-007-9177-9.

Green, M.A., Ho-Baillie, A., Snaith, H.J., 2014. The emergence of perovskite solar cells. Nat. Photonics 8, 506–514. https://doi.org/10.1038/nphoton.2014.134.

Ha, D., Fang, Z., Hu, L., Munday, J.N., 2014. Paper-based anti-reflection coatings for photovoltaics. Adv. Energy Mater. 4, 1301804. https://doi.org/10.1002/aenm.201301804.

Habisreutinger, S.N., Leijtens, T., Eperon, G.E., Stranks, S.D., Nicholas, R.J., Snaith, H.J., 2014a. Carbon nanotube/polymer composites as a highly stable hole collection layer in perovskite solar cells. Nano Lett. 14, 5561–5568. https://doi.org/10.1021/nl501982b.

Habisreutinger, S.N., Leijtens, T., Eperon, G.E., Stranks, S.D., Nicholas, R.J., Snaith, H.J., 2014b. Enhanced hole extraction in perovskite solar cells through carbon nanotubes. J. Phys. Chem. Lett. 5, 4207–4212. https://doi.org/10.1021/jz5021795.

Hagfeldt, A., Boschloo, G., Sun, L., Kloo, L., Pettersson, H., 2010. Dye-sensitized solar cells. Chem. Rev. 110, 6595–6663. https://doi.org/10.1021/cr900356p.

Hasan, O., Arif, A.F.M., 2014. Performance and life prediction model for photovoltaic modules: Effect of encapsulant constitutive behavior. Sol. Energy Mater. Sol. Cells 122, 75–87. https://doi.org/10.1016/j.solmat.2013.11.016.

Hashmi, S.G., Özkan, M., Halme, J., Zakeeruddin, S.M., Paltakari, J., Grätzel, M., Lund, P.D., 2016. Dye-sensitized solar cells with inkjet-printed dyes. Energy Environ. Sci. 9, 2453–2462. https://doi.org/10.1039/c6ee00826g.

Hayashi, K., Ishikawa, A., Endho, T., Yamagishi, H., 1994. New type of large-area a-Si module produced using a polymer encapsulation method. First WCPEC. 535–538.

Hayden, D.R., Mohan, S., Imhof, A., Velikov, K.P., 2019. Fully biobased highly transparent nanopaper with UV-blocking functionality. ACS Appl. Polym. Mater. 1, 641–646. https://doi.org/10.1021/acsapm.9b00192.

Hinsch, a., Kroon, J.M., Kern, R., Uhlendorf, I., Holzbock, J., Meyer, a., Ferber, J., 2001. Long-term stability of dye-sensitised solar cells. Prog. Photovoltaics Res. Appl. 9, 425–438. https://doi.org/10.1002/pip.397.

Hinsch, A., Behrens, S., Berginc, M., Bönnemann, H., Brandt, H., Drewitz, A., Einsele, F., Faßler, D., Gerhard, D., Gores, H., Haag, R., Herzig, T., Himmler, S., Khelashvili, G., Koch, D., Nazmutdinova, G., Opara-Krasovec, U., Putyra, P., Rau, U., Sastrawan, R., Schauer, T., Schreiner, C., Sensfuss, S., Siegers, C., Skupien, K., Wachter, P., Walter, J., Wasserscheid, P., Würfel, U., Zistler, M., 2008. Material development for dye solar modules: results from an integrated approach. Prog. Photovoltaics Res. Appl. 16, 489–501. https://doi.org/10.1002/pip.832.

Hirschl, C., Biebl-Rydlo, M., Debiasio, M., Mühleisen, W., Neumaier, L., Scherf, W., Oreski, G., Eder, G., Chernev, B., Schwab, W., Kraft, M., 2013. Determining the degree of crosslinking of ethylene vinyl acetate photovoltaic module encapsulants – a comparative study. Sol. Energy Mater. Sol. Cells 116, 203–218. https://doi.org/10.1016/j.solmat.2013.04.022.

Hoke, E.T., Slotcavage, D.J., Dohner, E.R., Bowring, A.R., Karunadasa, H.I., McGehee, M. D., 2015. Reversible photo-induced trap formation in mixed-halide hybrid perovskites for photovoltaics. Chem. Sci. 6, 613–617. https://doi.org/10.1039/c4sc03141e.

Holzhey, P., Saliba, M., 2018. A full overview of international standards assessing the long-term stability of perovskite solar cells. J. Mater. Chem. A 6, 21794–21808. https://doi.org/10.1039/C8TA06950F.

Hossain, L., Raghuwanshi, V.S., Tanner, J., Wu, C.-M., Kleinerman, O., Cohen, Y., Garnier, G., 2020. Structure and swelling of cross-linked nanocellulose foams. J. Colloid Interface Sci. 568, 234–244. https://doi.org/10.1016/j.jcis.2020.02.048.

Hosseinian Ahangharnejhad, R., Song, Z., Mariam, T., Gardner, J.J., Liyanage, G.K., Almutawah, Z.S., Anwar, B.M.M., Junda, M., Podraza, N.J., Phillips, A.B., Yan, Y., Heben, M.J., 2021. Protecting perovskite solar cells against moisture-induced degradation with sputtered inorganic barrier layers. ACS Appl. Energy Mater. 4, 7571–7578. https://doi.org/10.1021/acsaem.1c00816.

Hou, G., Liu, Y., Zhang, D., Li, G., Xie, H., Fang, Z., 2020. Approaching theoretical haze of highly transparent all-cellulose composite films. ACS Appl. Mater. Interfaces 12, 31998–32005. https://doi.org/10.1021/acsami.0c08586.

Huang, X., Han, S., Huang, W., Liu, X., 2013. Enhancing solar cell efficiency: the search for luminescent materials as spectral converters. Chem. Soc. Rev. 42, 173–201. https://doi.org/10.1039/C2CS35288E.

Huang, Z., Long, J., Dai, R., Hu, X., Le, L., Meng, X., Tan, L., Chen, Y., 2021. Ultra-flexible and waterproof perovskite photovoltaics for washable power source applications. Chem. Commun. 57, 6320–6323. https://doi.org/10.1039/d1cc01519b.

Huaulmé, Q., Mwalukuku, V.M., Joly, D., Liotier, J., Kervella, Y., Maldivi, P., Narbey, S., Oswald, F., Riquelme, A.J., Anta, J.A., Demadrille, R., 2020. Photochromic dye-sensitized solar cells with light-driven adjustable optical transmission and power conversion efficiency. Nat. Energy 5, 468–477. https://doi.org/10.1038/s41560-020-0624-7.

Hwang, I., Jeong, I., Lee, J., Ko, M.J., Yong, K., 2015. Enhancing stability of perovskite solar cells to moisture by the facile hydrophobic passivation. ACS Appl. Mater. Interfaces 7, 17330–17336. https://doi.org/10.1021/acsami.5b04490.

Idígoras, J., Aparicio, F.J., Contreras-Bernal, L., Ramos-Terrón, S., Alcaire, M., Sánchez-Valencia, J.R., Borras, A., Barranco, Á., Anta, J.A., 2018. Enhancing moisture and water resistance in perovskite solar cells by encapsulation with ultrathin plasma polymers. ACS Appl. Mater. Interfaces 10, 11587–11594. https://doi.org/10.1021/acsami.7b17824.

Ivanou, D.K., Santos, R., Maçaira, J., Andrade, L., Mendes, A., 2016. Laser assisted glass frit sealing for production large area DSCs panels. Sol. Energy 135, 674–681. https://doi.org/10.1016/j.solener.2016.06.043.

Jacobs, D.A., Langenhorst, M., Sahli, F., Richards, B.S., White, T.P., Ballif, C., Catchpole, K.R., Paetzold, U.W., 2019. Light management: a key concept in high-efficiency perovskite/silicon tandem photovoltaics. J. Phys. Chem. Lett. 10, 3159–3170. https://doi.org/10.1021/acs.jpclett.8b03721.

Jacobsson, J.T., Correa Baena, J.P., Pazoki, M., Saliba, M., Schenk, K., Grätzel, M., Hagfeldt, A., 2016. An exploration of the compositional space for mixed lead halogen perovskites for high efficiency devices. Energy Environ. Sci. https://doi.org/10.1039/C6EE00030D.

Jacucci, G., Schertel, L., Zhang, Y., Yang, H., Vignolini, S., 2020. Light management with natural materials: from whiteness to transparency. Adv. Mater. 2001215 https://doi.org/10.1002/adma.202001215.

Jang, J.H., Kim, B.J., Kim, J.H., Han, E., Choi, E.Y., Ji, C.H., Kim, K.T., Kim, J., Park, N., 2019. A novel approach for the development of moisture encapsulation poly(vinyl alcohol- co-ethylene) for perovskite solar cells. ACS Omega 4, 9211–9218. https://doi.org/10.1021/acsomega.9b00350.

Jeng, J.Y., Chen, K.C., Chiang, T.Y., Lin, P.Y., Tsai, T.D., Chang, Y.C., Guo, T.F., Chen, P., Wen, T.C., Hsu, Y.J., 2014. Nickel oxide electrode interlayer in CH3NH3PbI3perovskite/PCBM planar-heterojunction hybrid solar cells. Adv. Mater. 26, 4107–4113. https://doi.org/10.1002/adma.201306217.

Jeon, N.J., Noh, J.H., Kim, Y.C., Yang, W.S., Ryu, S., Seok, S.I., 2014. Solvent engineering for high-performance inorganic-organic hybrid perovskite solar cells. Nat. Mater. 13, 1–7. https://doi.org/10.1038/nmat4014.

Jeon, N.J., Noh, J.H., Yang, W.S., Kim, Y.C., Ryu, S., Seo, J., Sang, I., 2015. Compositional engineering of perovskite materials for high-performance solar cells. Nature 517, 476–480. https://doi.org/10.1038/nature14133.

Jeong, E.G., Jeon, Y., Cho, S.H., Choi, K.C., 2019. Textile-based washable polymer solar cells for optoelectronic modules: toward self-powered smart clothing. Energy Environ. Sci. 12, 1878–1889. https://doi.org/10.1039/c8ee03271h.

Jeong, M., Choi, I.W., Go, E.M., Cho, Y., Kim, M., Lee, B., Jeong, S., Jo, Y., Choi, H.W., Lee, J., Bae, J., Kwak, S.K., Kim, D.S., Yang, C., 2020. Stable perovskite solar cells with efficiency exceeding 24.8% and 0.3-V voltage loss. Science (80-.) 369, 1615–1620.

Jiang, Q., Zhang, X., You, J., 2018. SnO2: a wonderful electron transport layer for perovskite solar cells. Small 14, 1–14. https://doi.org/10.1002/smll.201801154.

Jiang, Y., Qiu, L., Juarez-Perez, E.J., Ono, L.K., Hu, Z., Liu, Z., Wu, Z., Meng, L., Wang, Q., Qi, Y., 2019. Reduction of lead leakage from damaged lead halide perovskite solar modules using self-healing polymer-based encapsulation. Nat. Energy 4, 585–593. https://doi.org/10.1038/s41560-019-0406-2.

Jo, Y., Jung, C., Lim, J., Kim, B.H., Han, C.-H., Kim, J., Kim, S., Kim, D., Jun, Y., 2012. A novel dye coating method for N719 dye-sensitized solar cells. Electrochim. Acta 66, 121–125. https://doi.org/10.1016/j.electacta.2012.01.055.

Jošt, M., Lipovšek, B., Glažar, B., Al-Ashouri, A., Brecl, K., Matič, G., Magomedov, A., Getautis, V., Topič, M., Albrecht, S., 2020. Perovskite Solar Cells go Outdoors: Field Testing and Temperature Effects on Energy Yield. Adv. Energy Mater. https://doi.org/10.1002/aenm.202000454.

Juillard, S., Planes, E., Matheron, M., Perrin, L., Berson, S., Flandin, L., 2018. Mechanical reliability of flexible encapsulated organic solar cells: characterization and improvement. ACS Appl. Mater. Interfaces 10, 29805–29813. https://doi.org/10.1021/acsami.8b06684.

Jung, Y.S., Hwang, K., Heo, Y.J., Kim, J.E., Vak, D., Kim, D.Y., 2018. Progress in scalable coating and roll-to-roll compatible printing processes of perovskite solar cells toward realization of commercialization. Adv. Opt. Mater. 6, 1–30. https://doi.org/10.1002/adom.201701182.

Kakiage, K., Aoyama, Y., Yano, T., Oya, K., Fujisawa, J., Hanaya, M., 2015. Highly-efficient dye-sensitized solar cells with collaborative sensitization by silyl-anchor and carboxy-anchor dyes. Chem. Commun. 51, 15894–15897. https://doi.org/10.1039/C5CC06759F.

Kamino, B.A., Paviet-Salomon, B., Moon, S.J., Badel, N., Levrat, J., Christmann, G., Walter, A., Faes, A., Ding, L., Diaz Leon, J.J., Paracchino, A., Despeisse, M., Ballif, C., Nicolay, S., 2019. Low-temperature screen-printed metallization for the scale-up of two-terminal perovskite-silicon tandems. ACS Appl. Energy Mater. 2, 3815–3821. https://doi.org/10.1021/acsaem.9b00502.

Kang, J.-G., Kim, J.-H., Jang, H.-B., Kim, J.-T., 2015. Characteristics of DSSC panels with silicone encapsulant. Int. J. Photoenergy 2015, 1–7. https://doi.org/10.1155/2015/715427.

Kawata, K., Tamaki, K., Kawaraya, M., 2015. Dye-sensitised and perovskite solar cells as indoor energy harvestors. J. Photopolym. Sci. Technol. 28, 415–417. https://doi.org/10.2494/photopolymer.28.415.

Kempe, M., 2011. Overview of scientific issues involved in selection of polymers for PV applications. Conf. Rec. IEEE Photovolt. Spec. Conf. 000085–000090 https://doi.org/10.1109/PVSC.2011.6185851.

Kempe, M.D., 2006. Modeling of rates of moisture ingress into photovoltaic modules. Sol. Energy Mater. Sol. Cells 90, 2720–2738. https://doi.org/10.1016/j.solmat.2006.04.002.

Kempe, M.D., Kilkenny, M., Moricone, T.J., Zhang, J.Z., 2009. Accelerated Stress Testing of Hydrocarbon-Based Encapsulants for Medium-Concentration CPV Applications, in: 2009 34th IEEE Photovoltaic Specialists Conference. IEEE, pp. 1826–1831.

Kempe, M.D., Miller, D.C., Wohlgemuth, J.H., Kurtz, S.R., Moseley, J.M., Nobles, D. l, Stika, K.M., Brun, Y., Samuels, S.L., Shah, Q.A., Tamizhmani, G., Sakurai, K., Inoue, M., Doi, T., Masuda, A., Vanderpan, C.E., 2016. Multi angle laser light scattering evaluation of field exposed thermoplastic photovoltaic encapsulant materials. Energy Sci. Eng. 4, 40–51. https://doi.org/10.1002/ese3.106.

Khadka, D.B., Shirai, Y., Yanagida, M., Miyano, K., 2017. Degradation of encapsulated perovskite solar cells driven by deep trap states and interfacial deterioration. J. Mater. Chem. C 6, 162–170. https://doi.org/10.1039/c7tc03733c.

Khare, A., 2020. A critical review on the efficiency improvement of upconversion assisted solar cells. J. Alloys Compd. 821, 153214 https://doi.org/10.1016/j.jallcom.2019.153214.

Khenkin, M. V., Katz, E.A., Abate, A., Bardizza, G., Berry, J.J., Brabec, C., Brunetti, F., Bulović, V., Burlingame, Q., Di Carlo, A., Cheacharoen, R., Cheng, Y.B., Colsmann, A., Cros, S., Domanski, K., Dusza, M., Fell, C.J., Forrest, S.R., Galagan, Y., Di Girolamo, D., Grätzel, M., Hagfeldt, A., von Hauff, E., Hoppe, H., Kettle, J., Köbler, H., Leite, M.S., Liu, S. (Frank), Loo, Y.L., Luther, J.M., Ma, C.Q., Madsen, M., Manceau, M., Matheron, M., McGehee, M., Meitzner, R., Nazeeruddin, M.K., Nogueira, A.F., Odabaşı, Ç., Osherov, A., Park, N.G., Reese, M.O., De Rossi, F., Saliba, M., Schubert, U.S., Snaith, H.J., Stranks, S.D., Tress, W., Troshin, P.A., Turkovic, V., Veenstra, S., Visoly-Fisher, I., Walsh, A., Watson, T., Xie, H., Yıldırım, R., Zakeeruddin, S.M., Zhu, K., Lira-Cantu, M., 2020. Consensus statement for stability assessment and reporting for perovskite photovoltaics based on ISOS procedures. Nat. Energy 5, 35–49. https://doi.org/10.1038/s41560-019-0529-5.

Kim, B.J., Jang, J.H., Kim, J., Oh, K.S., Choi, E.Y., Park, N., 2019a. Efficiency and stability enhancement of organic–inorganic perovskite solar cells through micropatterned Norland Optical Adhesive and polyethylene terephthalate encapsulation. Mater. Today Commun. 20, 100537 https://doi.org/10.1016/j.mtcomm.2019.05.013.

Kim, H.-S., Lee, C.-R., Im, J.-H., Lee, K.-B., Moehl, T., Marchioro, A., Moon, S.-J., Humphry-Baker, R., Yum, J.-H., Moser, J.E., Grätzel, M., Park, N.-G., 2012. Lead iodide perovskite sensitized all-solid-state submicron thin film mesoscopic solar cell with efficiency exceeding 9%. Sci. Rep. 2, 591. https://doi.org/10.1038/srep00591.

Kim, H., Lee, J., Kim, B., Byun, H.R., Kim, S.H., Oh, H.M., Baik, S., Jeong, M.S., 2019b. Enhanced stability of MAPbI3 perovskite solar cells using poly(p-chloro-xylylene) encapsulation. Sci. Rep. 9, 1–6. https://doi.org/10.1038/s41598-019-51945-9.

Kim, M., Kim, G.H., Lee, T.K., Choi, I.W., Choi, H.W., Jo, Y., Yoon, Y.J., Kim, J.W., Lee, J., Huh, D., Lee, H., Kwak, S.K., Kim, J.Y., Kim, D.S., 2019c. Methylammonium chloride induces intermediate phase stabilization for efficient perovskite solar cells. Joule 3, 2179–2192. https://doi.org/10.1016/j.joule.2019.06.014.

Kim, M.S., Lee, J.H., Kwak, M.K., 2020. Review: surface texturing methods for solar cell efficiency enhancement. Int. J. Precis. Eng. Manuf. 21, 1389–1398. https://doi.org/10.1007/s12541-020-00337-5.

Knechtel, R., 2005. Glass frit bonding: an universal technology for wafer level encapsulation and packaging. Microsyst. Technol. 12, 63–68. https://doi.org/10.1007/s00542-005-0022-x.

Kovrov, A., Helgesen, M., Boeffel, C., Kröpke, S., Søndergaard, R.R., 2020. Novel acrylic monomers for organic photovoltaics encapsulation. Sol. Energy Mater. Sol. Cells 204, 1–9. https://doi.org/10.1016/j.solmat.2019.110210.

Kraft, A., Labusch, L., Ensslen, T., Durr, I., Bartsch, J., Glatthaar, M., Glunz, S., Reinecke, H., 2015. Investigation of acetic acid corrosion impact on printed solar cell contacts. IEEE J. Photovoltaics 5, 736–743. https://doi.org/10.1109/JPHOTOV.2015.2395146.

Krebs, F.C., 2006. Encapsulation of polymer photovoltaic prototypes. Sol. Energy Mater. Sol. Cells 90, 3633–3643. https://doi.org/10.1016/j.solmat.2006.06.055.

Lan, J.L., Wei, T.C., Feng, S.P., Wan, C.C., Cao, G., 2012. Effects of iodine content in the electrolyte on the charge transfer and power conversion efficiency of dye-sensitized solar cells under low light intensities. J. Phys. Chem. C 116, 25727–25733. https://doi.org/10.1021/jp309872n.

Lange, R.F.M., Luo, Y., Polo, R., Zahnd, J., 2011. The lamination of (multi)crystalline and thin film based photovoltaic modules. Prog. Photovoltaics Res. Appl. 19, 127–133. https://doi.org/10.1002/pip.993.

Lee, H.J., Kim, H.P., Kim, H.M., Youn, J.H., Nam, D.H., Lee, Y.G., Lee, J.G., Mohd Yusoff, A.R. Bin, Jang, J., 2013a. Solution processed encapsulation for organic photovoltaics. Sol. Energy Mater. Sol. Cells 111, 97–101. https://doi.org/10.1016/j.solmat.2012.12.041.

Lee, I., Hwang, S., Kim, H., 2011. Reaction between oxide sealant and liquid electrolyte in dye-sensitized solar cells. Sol. Energy Mater. Sol. Cells 95, 315–317. https://doi.org/10.1016/j.solmat.2010.04.052.

Lee, J.W., Kim, S.G., Yang, J.M., Yang, Y., Park, N.G., 2019. Verification and mitigation of ion migration in perovskite solar cells. APL Mater. 7 https://doi.org/10.1063/1.5085643.

Lee, M.M., Teuscher, J., Miyasaka, T., Murakami, T.N., Snaith, H.J., 2012. Efficient hybrid solar cells based on meso-superstructured organometal halide perovskites. Science (80-.) 338, 643–647.

Leijtens, T., Eperon, G.E., Pathak, S., Abate, A., Lee, M.M., Snaith, H.J., 2013. Overcoming ultraviolet light instability of sensitized TiO2 with meso-superstructured organometal tri-halide perovskite solar cells. Nat. Commun. 4, 1–8. https://doi.org/10.1038/ncomms3885.

Lertngim, A., Phiriyawirut, M., Wootthikanokkhan, J., Yuwawech, K., Sangkhun, W., Kumnorkaew, P., Muangnapoh, T., 2017. Preparation of Surlyn films reinforced with cellulose nanofibres and feasibility of applying the transparent composite films for organic photovoltaic encapsulation. R. Soc. Open Sci. 4, 170792 https://doi.org/10.1098/rsos.170792.

Li, B., Wang, M., Subair, R., Cao, G., Tian, J., 2018a. Significant stability enhancement of perovskite solar cells by facile adhesive encapsulation. J. Phys. Chem. C 122, 25260–25267. https://doi.org/10.1021/acs.jpcc.8b09595.

Li, W., Liu, Q., Zhang, Y., Li, C., He, Z., Choy, W.C.H., Low, P.J., Sonar, P., Kyaw, A.K.K., 2020. Biodegradable materials and green processing for green electronics. Adv. Mater. 32, 2001591. https://doi.org/10.1002/adma.202001591.

Li, X., Tschumi, M., Han, H., Babkair, S.S., Alzubaydi, R.A., Ansari, A.A., Habib, S.S., Nazeeruddin, M.K., Zakeeruddin, S.M., Grätzel, M., 2015. Outdoor performance and stability under elevated temperatures and long-term light soaking of triple-layer mesoporous perovskite photovoltaics. Energy Technol. 3, 551–555. https://doi.org/10.1002/ente.201500045.

Li, Y., Cheng, M., Jungstedt, E., Xu, B., Sun, L., Berglund, L., 2019. Optically transparent wood substrate for perovskite solar cells. ACS Sustain. Chem. Eng. 7, 6061–6067. https://doi.org/10.1021/acssuschemeng.8b06248.

Li, Y., Tsai, C., Kao, S., Wu, I., Chen, J., Wu, C., Lin, C.-F., Cheng, I.-C., 2013. Single-layer organic-inorganic-hybrid thin-film encapsulation for organic solar cells. J. Phys. D Appl. Phys. 46, 435502 https://doi.org/10.1088/0022-3727/46/43/435502.

Li, Y., Vasileva, E., Sychugov, I., Popov, S., Berglund, L., 2018b. Optically transparent wood: recent progress, opportunities, and challenges. Adv. Opt. Mater. 6, 1800059. https://doi.org/10.1002/adom.201800059.

Liu, M., Johnston, M.B., Snaith, H.J., 2013. Efficient planar heterojunction perovskite solar cells by vapour deposition. Nature 501, 395–398. https://doi.org/10.1038/nature12509.

López-Escalante, M.C., Caballero, L.J., Martín, F., Gabás, M., Cuevas, A., Ramos-Barrado, J.R., 2016. Polyolefin as PID-resistant encapsulant material in PV modules. Sol. Energy Mater. Sol. Cells 144, 691–699. https://doi.org/10.1016/j.solmat.2015.10.009.

Luo, J., Yang, H.B., Zhuang, M., Liu, S., Wang, L., Liu, B., 2020. Making fully printed perovskite solar cells stable outdoor with inorganic superhydrophobic coating. J. Energy Chem. 50, 332–338. https://doi.org/10.1016/j.jechem.2020.03.082.

Lv, Y., Zhang, H., Liu, R., Sun, Y., Huang, W., 2020. Composite encapsulation enabled superior comprehensive stability of perovskite solar cells. ACS Appl. Mater. Interfaces 12, 27277–27285. https://doi.org/10.1021/acsami.0c06823.

Ma, S., Bai, Y., Wang, H., Zai, H., Wu, J., Li, L., Xiang, S., Liu, N., Liu, L., Zhu, C., Liu, G., Niu, X., Chen, H., Zhou, H., Li, Y., Chen, Q., 2020. 1000 h operational lifetime perovskite solar cells by ambient melting encapsulation. Adv. Energy Mater. 10, 1902472. https://doi.org/10.1002/aenm.201902472.

Malinauskas, T., Tomkute-Luksiene, D., Sens, R., Daskeviciene, M., Send, R., Wonneberger, H., Jankauskas, V., Bruder, I., Getautis, V., 2015. Enhancing thermal stability and lifetime of solid-state dye-sensitized solar cells via molecular engineering of the hole-transporting material spiro-OMeTAD. ACS Appl. Mater. Interfaces 7, 11107–11116. https://doi.org/10.1021/am5090385.

Mariani, P., Vesce, L., Di Carlo, A., 2015. The role of printing techniques for large-area dye sensitized solar cells. Semicond. Sci. Technol 30, 104003. https://doi.org/10.1088/0268-1242/30/10/104003.

Martins, J., Emami, S., Madureira, R., Mendes, J., Ivanou, D., Mendes, A., 2020. Novel laser-assisted glass frit encapsulation for long-lifetime perovskite solar cells. J. Mater. Chem. A 8, 20037–20046. https://doi.org/10.1039/d0ta05583b.

Mastroianni, S., Asghar, I., Miettunen, K., Halme, J., Lanuti, A., Brown, T.M., Lund, P., 2014. Effect of electrolyte bleaching on the stability and performance of dye solar cells. Phys. Chem. Chem. Phys. 16, 6092–6100. https://doi.org/10.1039/C3CP55342F.

Mathew, S., Yella, A., Gao, P., Humphry-Baker, R., Curchod, B.F.E., Ashari-Astani, N., Tavernelli, I., Rothlisberger, U., Nazeeruddin, M.K., Grätzel, M., 2014. Dye-sensitized solar cells with 13% efficiency achieved through the molecular engineering of porphyrin sensitizers. Nat. Chem. 6, 242–247. https://doi.org/10.1038/nchem.1861.

Matteocci, F., Cinà, L., Lamanna, E., Cacovich, S., Divitini, G., Midgley, P.A., Ducati, C., Di Carlo, A., 2016. Encapsulation for long-term stability enhancement of perovskite solar cells. Nano Energy 30, 162–172. https://doi.org/10.1016/j.nanoen.2016.09.041.

Meng, L., Zhang, Y., Wan, X., Li, C., Zhang, X., Wang, Y., Ke, X., Xiao, Z., Ding, L., Xia, R., Yip, H.L., Cao, Y., Chen, Y., 2018. Organic and solution-processed tandem solar cells with 17.3% efficiency. Science (80-.) 361, 1094–1098. https://doi.org/10.1126/science.aat2612.

Mi, R., Li, T., Dalgo, D., Chen, C., Kuang, Y., He, S., Zhao, X., Xie, W., Gan, W., Zhu, J., Srebric, J., Yang, R., Hu, L., 2020. A clear, strong, and thermally insulated transparent wood for energy efficient windows. Adv. Funct. Mater. 30, 1907511. https://doi.org/10.1002/adfm.201907511.

Miettunen, K., Vapaavuori, J., Tiihonen, A., Poskela, A., Lahtinen, P., Halme, J., Lund, P., 2014. Nanocellulose aerogel membranes for optimal electrolyte fi lling in dye solar cells. Nano Energy 8, 95–102. https://doi.org/10.1016/j.nanoen.2014.05.013.

Miller, D.C., Kempe, M.D., Glick, S.H., Kurtz, S.R., 2010. Creep in photovoltaic modules: examining the stability of polymeric materials and components. Conf. Rec. IEEE Photovolt. Spec. Conf. 262–268 https://doi.org/10.1109/PVSC.2010.5615832.

Moffatt, J.E., Tsiminis, G., Klantsataya, E., de Prinse, T.J., Ottaway, D., Spooner, N.A., 2020. A practical review of shorter than excitation wavelength light emission processes. Appl. Spectrosc. Rev. 55, 327–349. https://doi.org/10.1080/05704928.2019.1672712.

Myong, S.Y., Park, J.H., Kwon, S.W., 2014. Inferior outdoor-exposed performances of encapsulated a-si: H photovoltaic modules deposited with a high speed. Energy Sci. Eng. 2, 14–21. https://doi.org/10.1002/ese3.26.

Nagayama, K., Kapur, J., Morris, B.A., 2020. Influence of two-phase behavior of ethylene ionomers on diffusion of water. J. Appl. Polym. Sci. 137, 1–9. https://doi.org/10.1002/app.48929.

Nakajima, S., Katoh, R., 2015. Mechanism of degradation of electrolyte solutions for dye-sensitized solar cells under ultraviolet light irradiation. Chem. Phys. Lett. 619, 36–38. https://doi.org/10.1016/j.cplett.2014.11.035.

Nath, N.C.D., Lee, H.Y., Son, Y., Lee, J.-J., 2017. Ethylene-polypropylene copolymer as an effective sealing spacer for dye-sensitized solar cells. J. Nanosci. Nanotechnol. 17, 8045–8052. https://doi.org/10.1166/jnn.2017.15101.

Nelson, J., 2011. Polymer: fullerene bulk heterojunction solar cells. Mater. Today 14, 462–470. https://doi.org/10.1016/S1369-7021(11)70210-3.

Nguyen, T.D., Hamad, W.Y., MacLachlan, M.J., 2017. Near-IR-sensitive upconverting nanostructured photonic cellulose films. Adv. Opt. Mater. 5, 1–7. https://doi.org/10.1002/adom.201600514.

Nikafshar, S., Zabihi, O., Ahmadi, M., Mirmohseni, A., Taseidifar, M., Naebe, M., 2017. The effects of UV light on the chemical and mechanical properties of a transparent epoxy-diamine system in the presence of an organic UV absorber. Materials (Basel) 10, 180. https://doi.org/10.3390/ma10020180.

Nonat, A., Fix, T., 2019. Photon Converters for Photovoltaics, in: Advanced Micro- and Nanomaterials for Photovoltaics. Elsevier, pp. 121–151. https://doi.org/10.1016/B978-0-12-814501-2.00006-2.

NREL, 2020. NREL Best Research - Solar Cell Efficiencies [WWW Document]. URL https://www.nrel.gov/pv/cell-efficiency.html.

O'Regan, B., Grätzel, M., 1991. A low-cost, high-efficiency solar cell based on dye-sensitized colloidal TiO_2 films. Nature 353, 737–740. https://doi.org/10.1038/353737a0.

Olsen, L.C., Gross, M.E., Graff, G.L., Kundu, S.N., Chu, X., Lin, S., 2008. Approaches to encapsulation of flexible CIGS cells. Reliab. Photovolt. Cells, Modul. Components, Syst. 7048, 70480O. https://doi.org/10.1117/12.796104.

Olsen, L.C., Kundu, S.N., Bonham, C.C., Gross, M., 2005. Barrier coatings for CIGSS and CdTe cells. Conference Record of the Thirty-First IEEE Photovoltaic Specialists Conference. 327–330.

Osayemwenre, G.O., Meyer, E.L., 2014. Thermal decomposition of eva composite encapsulant of single junction amorphous silicon photovoltaic (Pv) module. J. Ovonic Res. 10, 221–229.

Parel, T.S., Danos, L., Markvart, T., 2015. Application of concentrating luminescent down-shifting structures to CdS/CdTe solar cells with poor short wavelength response. Sol. Energy Mater. Sol. Cells 140, 306–311. https://doi.org/10.1016/j.solmat.2015.04.026.

Park, B.W., Philippe, B., Zhang, X., Rensmo, H., Boschloo, G., Johansson, E.M.J., 2015. Bismuth based hybrid perovskites A3Bi2I9 (A: methylammonium or cesium) for solar cell application. Adv. Mater. 27, 6806–6813. https://doi.org/10.1002/adma.201501978.

Patel, A.P., Sinha, A., Tamizhmani, G., 2020. Field-aged glass/backsheet and glass/glass PV modules: encapsulant degradation comparison. IEEE J. Photovoltaics 10, 607–615. https://doi.org/10.1109/JPHOTOV.2019.2958516.

Peike, C., Hädrich, I., Weiß, K., Dürr, I., 2013. Overview of PV module encapsulation materials. Photovoltaics Int. 22, 85–92.

Pellet, N., Gao, P., Gregori, G., Yang, T.Y., Nazeeruddin, M.K., Maier, J., Gr??tzel, M., 2014. Mixed-organic-cation perovskite photovoltaics for enhanced solar-light harvesting. Angew. Chemie - Int. Ed. 53, 3151–3157. https://doi.org/10.1002/anie.201309361.

Pern, F.J., Glick, S.H., 2000. Photothermal stability of encapsulated silicon solar cells and encapsulation materials upon accelerated exposures - II. Conf. Rec. IEEE Photovolt. Spec. Conf. 2000-Janua, 1491–1494. https://doi.org/10.1109/PVSC.2000.916176.

Photovoltaics Report - Fraunhofer ISE, 2020. , Fraunhofer Istitute for solar energy systems ISE.

Podsiadlo, P., Sui, L., Elkasabi, Y., Burgardt, P., Lee, J., Miryala, A., Kusumaatmaja, W., Carman, M.R., Shtein, M., Kieffer, J., Lahann, J., Kotov, N.A., 2007. Layer-by-layer assembled films of cellulose nanowires with antireflective properties. Langmuir 23, 7901–7906. https://doi.org/10.1021/la700772a.

Poskela, A., Miettunen, K., Borghei, M., Vapaavuori, J., Greca, L.G., Lehtonen, J., Solin, K., Ago, M., Lund, P.D., Rojas, O.J., 2019. Nanocellulose and nanochitin cryogels improve the efficiency of dye solar cells. ACS Sustain. Chem. Eng. 7, 10257–10265. https://doi.org/10.1021/acssuschemeng.8b06501.

Poskela, A., Miettunen, K., Tiihonen, A., Lund, P.D., 2020. Extreme sensitivity of dye solar cells to UV-induced degradation. Energy Sci. Eng. 00, 1–8. https://doi.org/10.1002/ese3.810.

Rajamanickam, N., Kumari, S., Vendra, V.K., Lavery, B.W., Spurgeon, J., Druffel, T., Sunkara, M.K., 2016. Stable and durable CH3NH3PbI3 perovskite solar cells at ambient conditions. Nanotechnology 27. https://doi.org/10.1088/0957-4484/27/23/235404.

Rajeswari, R., Islavath, N., Raghavender, M., Giribabu, L., 2020. Recent progress and emerging applications of rare earth doped phosphor materials for dye-sensitized and perovskite solar cells: a review. Chem. Rec. 20, 65–88. https://doi.org/10.1002/tcr.201900008.

Rajput, P., Malvoni, M., Kumar, N.M., Sastry, O.S., Tiwari, G.N., 2019. Risk priority number for understanding the severity of photovoltaic failure modes and their impacts on performance degradation. Case Stud. Therm. Eng. 16, 100563 https://doi.org/10.1016/j.csite.2019.100563.

Ramasamy, E., Karthikeyan, V., Rameshkumar, K., Veerappan, G., 2019. Glass-to-glass encapsulation with ultraviolet light curable epoxy edge sealing for stable perovskite solar cells. Mater. Lett. 250, 51–54. https://doi.org/10.1016/j.matlet.2019.04.082.

Ribeiro, F., MaçAira, J., Cruz, R., Gabriel, J., Andrade, L., Mendes, A., 2012. Laser assisted glass frit sealing of dye-sensitized solar cells. Sol. Energy Mater. Sol. Cells 96, 43–49. https://doi.org/10.1016/j.solmat.2011.09.009.

Rizzo, A., Ortolan, L., Murrone, S., Torto, L., Barbato, M., Wrachien, N., Cester, A., Matteocci, F., Di Carlo, A., 2017. Effects of thermal stress on hybrid perovskite solar cells with different encapsulation techniques. IEEE Int. Reliab. Phys. Symp. Proc. PV1.1-PV1.6 https://doi.org/10.1109/IRPS.2017.7936396.

Ross, D., Alonso-Álvarez, D., Klampaftis, E., Fritsche, J., Bauer, M., Debije, M.G., Fifield, R.M., Richards, B.S., 2014. The impact of luminescent down shifting on the

performance of cdte photovoltaics: impact of the module vintage. IEEE J. Photovoltaics 4, 457–464. https://doi.org/10.1109/JPHOTOV.2013.2282896.
Roy, P., Kumar Sinha, N., Tiwari, S., Khare, A., 2020. A review on perovskite solar cells: evolution of architecture, fabrication techniques, commercialization issues and status. Sol. Energy 198, 665–688. https://doi.org/10.1016/j.solener.2020.01.080.
Sadeghifar, H., Ragauskas, A., 2020. Lignin as a UV light blocker—a review. Polymers (Basel). 12, 1134. https://doi.org/10.3390/polym12051134.
Saliba, M., Matsui, T., Domanski, K., Seo, J.-Y., Ummadisingu, A., Zakeeruddin, S.M., Correa-Baena, J.-P., Tress, W.R., Abate, A., Hagfeldt, A., Gratzel, M., 2016a. Incorporation of rubidium cations into perovskite solar cells improves photovoltaic performance. Science (80-.) 354, 206–209. https://doi.org/10.1126/science.aah5557.
Saliba, M., Matsui, T., Seo, J.-Y., Domanski, K., Correa-Baena, J.-P., Nazeeruddin, M.K., Zakeeruddin, S.M., Tress, W., Abate, A., Hagfeldt, A., Grätzel, M., 2016b. Cesium-containing triple cation perovskite solar cells: improved stability, reproducibility and high efficiency. Energy Environ. Sci. 9, 1989–1997. https://doi.org/10.1039/C5EE03874J.
Sastrawan, R., Beier, J., Belledin, U., Hemming, S., Hinsch, A., Kern, R., Vetter, C., Petrat, F.M., Prodi-Schwab, A., Lechner, P., Hoffmann, W., 2006a. A glass frit-sealed dye solar cell module with integrated series connections. Sol. Energy Mater. Sol. Cells 90, 1680–1691. https://doi.org/10.1016/j.solmat.2005.09.003.
Sastrawan, R., Beier, J., Belledin, U., Hemming, S., Hinsch, A., Kern, R., Vetter, C., Petrat, F.M., Prodi-Schwab, A., Lechner, P., Hoffmann, W., 2006b. New interdigital design for large area dye solar modules using a lead-free glass frit sealing. Prog. Photovoltaics Res. Appl. 14, 697–709. https://doi.org/10.1002/pip.700.
Schachinger, M., 2021. Module Price Index. PV Mag.
Shao, S., Liu, J., Portale, G., Fang, H.H., Blake, G.R., ten Brink, G.H., Koster, L.J.A., Loi, M.A., 2018. Highly reproducible Sn-based hybrid perovskite solar cells with 9% efficiency. Adv. Energy Mater. 8 https://doi.org/10.1002/aenm.201702019.
Shao, Y., Wang, Q., Dong, Q., Yuan, Y., Huang, J., 2015. Vacuum-free laminated top electrode with conductive tapes for scalable manufacturing of efficient perovskite solar cells. Nano Energy 16, 47–53. https://doi.org/10.1016/j.nanoen.2015.06.010.
Sharma, K., Sharma, V., Sharma, S.S., 2018. Dye-sensitized solar cells: fundamentals and current status. Nanoscale Res. Lett. 13, 381. https://doi.org/10.1186/s11671-018-2760-6.
Shen, T., Gnanakaran, S., 2009. The stability of cellulose: a statistical perspective from a coarse-grained model of hydrogen-bond networks. Biophys. J. 96, 3032–3040. https://doi.org/10.1016/j.bpj.2008.12.3953.
Shi, L., Bucknall, M.P., Young, T.L., Zhang, M., Hu, L., Bing, J., Lee, D.S., Kim, J., Wu, T., Takamure, N., McKenzie, D.R., Huang, S., Green, M.A., Ho-Baillie, A.W.Y., 2020. Gas chromatography–mass spectrometry analyses of encapsulated stable perovskite solar cells. Science (80-.) 2412, eaba2412. https://doi.org/10.1126/science.aba2412.
Shi, L., Young, T.L., Kim, J., Sheng, Y., Wang, L., Chen, Y., Feng, Z., Keevers, M.J., Hao, X., Verlinden, P.J., Green, M.A., Ho-Baillie, A.W.Y., 2017. Accelerated lifetime testing of organic-inorganic perovskite solar cells encapsulated by polyisobutylene. ACS Appl. Mater. Interfaces 9, 25073–25081. https://doi.org/10.1021/acsami.7b07625.
Smijs, T., Pavel, 2011. Titanium dioxide and zinc oxide nanoparticles in sunscreens: focus on their safety and effectiveness. Nanotechnol. Sci. Appl. 95. https://doi.org/10.2147/NSA.S19419.
Sommeling, P., Späth, M., Smit, H.J., Bakker, N., Kroon, J., 2004. Long-term stability testing of dye-sensitized solar cells. J. Photochem. Photobiol. A Chem. 164, 137–144. https://doi.org/10.1016/j.jphotochem.2003.12.017.
Son, M.-K., Seo, H., 2020. Effect of ultraviolet radiation on the long-term stability of dye-sensitized solar cells. Electron. Mater. Lett. 50, 71–73. https://doi.org/10.1007/s13391-020-00249-6.
Stoichkov, V., Bristow, N., Troughton, J., De Rossi, F., Watson, T.M., Kettle, J., 2018. Outdoor performance monitoring of perovskite solar cell mini-modules: diurnal performance, observance of reversible degradation and variation with climatic performance. Sol. Energy 170, 549–556. https://doi.org/10.1016/j.solener.2018.05.086.
Sun, S.-Y., Ge, Y.-Y., Zhao, Y.-J., Xie, Z.-P., 2021. Synthesis of Er3+ doped $KNbO_3$ nanocrystals and nanoceramics with outstanding up-conversion luminescence behaviors. J. Alloys Compd. 854, 156738 https://doi.org/10.1016/j.jallcom.2020.156738.
Sundaramoorthy, R., Pern, F.J., Gessert, T., 2010. Preliminary damp-heat stability studies of encapsulated CIGS solar cells. Reliab. Photovolt. Cells, Modul. Components, Syst. III 7773, 77730Q. https://doi.org/10.1117/12.863076.
Swonke, T., Auer, R., 2009. Impact of moisture on PV module encapsulants. Reliab. Photovolt. Cells, Modul. Components, Syst. II 7412, 74120A. https://doi.org/10.1117/12.825943.
Topolniak, I., Chapel, A., Gaume, J., Bussiere, P.O., Chadeyron, G., Gardette, J.L., Therias, S., 2017. Applications of polymer nanocomposites as encapsulants for solar cells and LEDs: impact of photodegradation on barrier and optical properties. Polym. Degrad. Stab. 145, 52–59. https://doi.org/10.1016/j.polymdegradstab.2017.06.013.
Tracy, J., Bosco, N., Delgado, C., Dauskardt, R., 2020. Durability of ionomer encapsulants in photovoltaic modules. Sol. Energy Mater. Sol. Cells 208, 110397. https://doi.org/10.1016/j.solmat.2020.110397.
Tripathi, N., Yanagida, M., Shirai, Y., Masuda, T., Han, L., Miyano, K., 2015. Hysteresis-free and highly stable perovskite solar cells produced via a chlorine-mediated interdiffusion method. J. Mater. Chem. A 3, 12081–12088. https://doi.org/10.1039/c5ta01668a.
Uddin, A., Upama, M.B., Yi, H., Duan, L., 2019. Encapsulation of organic and perovskite solar cells: a review. Coatings 9, 1–17. https://doi.org/10.3390/coatings9020065.
Vijayan, A., Johansson, M.B., Svanström, S., Cappel, U.B., Rensmo, H., Boschloo, G., 2020. Simple method for efficient slot-die coating of MAPbI3Perovskite thin films in ambient air conditions. ACS Appl. Energy Mater. 3, 4331–4337. https://doi.org/10.1021/acsaem.0c00039.
Visco, A., Scolaro, C., Iannazzo, D., Di Marco, G., 2019. Comparison of physical-mechanical features of polyethylene based polymers employed as sealants in solar cells. Int. J. Polym. Anal. Charact. 24, 97–104. https://doi.org/10.1080/1023666X.2018.1551267.
Wang, J., Xuan, Y., Da, Y., Xu, Y., Zheng, L., 2020. Benefits of photonic management strategy for highly efficient bifacial solar cells. Opt. Commun. 462, 125358 https://doi.org/10.1016/j.optcom.2020.125358.
Wang, M., Ma, P., Yin, M., Lu, L., Lin, Y., Chen, X., Jia, W., Cao, X., Chang, P., Li, D., 2017. Scalable production of mechanically robust antireflection film for omnidirectional enhanced flexible thin film solar cells. Adv. Sci. 4, 1700079. https://doi.org/10.1002/advs.201700079.
Wang, Q., Ito, S., Grätzel, M., Fabregat-Santiago, F., Mora-Seró, I., Bisquert, J., Bessho, T., Imai, H., 2006. Characteristics of high efficiency dye-sensitized solar cells. J. Phys. Chem. B 110, 25210–25221. https://doi.org/10.1021/jp064256o.
Wang, X., Tang, Q., He, B., Li, R., Yu, L., 2015. 7.35% Efficiency rear-irradiated flexible dye-sensitized solar cells by sealing liquid electrolyte in a groove. Chem. Commun. 51, 491–494. https://doi.org/10.1039/c4cc07549h.
Weerasinghe, H.C., Dkhissi, Y., Scully, A.D., Caruso, R.A., Cheng, Y.B., 2015. Encapsulation for improving the lifetime of flexible perovskite solar cells. Nano Energy 18, 118–125. https://doi.org/10.1016/j.nanoen.2015.10.006.
Wilson, G.M., Al-Jassim, M., Metzger, W.K., Glunz, S.W., Verlinden, P., Xiong, G., Mansfield, L.M., Stanbery, B.J., Zhu, K., Yan, Y., Berry, J.J., Ptak, A.J., Dimroth, F., Kayes, B.M., Tamboli, A.C., Peibst, R., Catchpole, K., Reese, M.O., Klinga, C.S., Denholm, P., Morjaria, M., Deceglie, M.G., Freeman, J.M., Mikofski, M.A., Jordan, D.C., Tamizhmani, G., Sulas-Kern, D.B., 2020. The 2020 photovoltaic technologies roadmap. J. Phys. D. Appl. Phys. 53 https://doi.org/10.1088/1361-6463/ab9c6a.
Wojciechowski, K., Leijtens, T., Siprova, S., Schlueter, C., Hörantner, M.T., Wang, J.T.W., Li, C.Z., Jen, A.K.Y., Lee, T.L., Snaith, H.J., 2015a. C_{60} as an efficient n-type compact layer in perovskite solar cells. J. Phys. Chem. Lett. 6, 2399–2405. https://doi.org/10.1021/acs.jpclett.5b00902.
Wojciechowski, K., Leijtens, T., Siprova, S., Schlueter, C., Hörantner, M.T., Wang, J.T.W., Li, C.Z., Jen, A.K.Y., Lee, T.L., Snaith, H.J., 2015b. C60 as an efficient n-type compact layer in perovskite solar cells. J. Phys. Chem. Lett. 6, 2399–2405. https://doi.org/10.1021/acs.jpclett.5b00902.
Wu, J., Che, X., Hu, H.-C., Xu, H., Li, B., Liu, Y., Li, J., Ni, Y., Zhang, X., Ouyang, X., 2020. Organic solar cells based on cellulose nanopaper from agroforestry residues with an efficiency of over 16% and effectively wide-angle light capturing. J. Mater. Chem. A 8, 5442–5448. https://doi.org/10.1039/C9TA14039E.
Xu, L., 2017. Efficiency loss of thin film Cu(InxGa1-x)Se(S) solar panels by lamination process. J. Appl. Phys. 121 https://doi.org/10.1063/1.4979635.
Yang, J., Min, M., Yoon, Y., Kim, W.J., Kim, S., Lee, H., 2016. Impermeable flexible liquid barrier film for encapsulation of DSSC metal electrodes. Sci. Rep. 6, 27422. https://doi.org/10.1038/srep27422.
Yang, J., Siempelkamp, B.D., Liu, D., Kelly, T.L., 2015. Investigation of CH3NH3PbI3 degradation rates and mechanisms in controlled humidity environments using in situ techniques. ACS Nano 9, 1955–1963. https://doi.org/10.1021/nn506864k.
Yang, K.Y., Kim, J., Cho, H.K., Ha, T.J., Kim, Y.H., 2017. Environment-stable solar window modules encapsulated with UV-curable transparent resin. Sol. Energy 158, 528–532. https://doi.org/10.1016/j.solener.2017.10.002.
Yeoh, M.E., Jaloman, A., Chan, K.Y., 2019. Aging effect in dye-sensitized solar cells sealed with thermoplastic films. Microelectron. Int. 36, 68–72. https://doi.org/10.1108/MI-11-2018-0075.
Yun, M.J., Sim, Y.H., Lee, D.Y., Cha, S.I., 2020a. Omni-directional light capture in PERC solar cells enhanced by stamping hierarchical structured silicone encapsulation that mimics leaf epidermis. RSC Adv. 10, 34837–34846. https://doi.org/10.1039/D0RA03378B.
Yun, M.J., Sim, Y.H., Lee, D.Y., Cha, S.I., 2020b. Omni-direction PERC solar cells harnessing periodic locally focused light incident through patterned PDMS encapsulation. RSC Adv. 10, 12415–12422. https://doi.org/10.1039/D0RA00439A.
Yun, S., Freitas, J.N., Nogueira, A.F., Wang, Y., Ahmad, S., Wang, Z.S., 2016. Dye-sensitized solar cells employing polymers. Prog. Polym. Sci. 59, 1–40. https://doi.org/10.1016/j.progpolymsci.2015.10.004.
Yuwawech, K., Wootthikanokkhan, J., Tanpichai, S., 2018. Transparency, moisture barrier property, and performance of the alternative solar cell encapsulants based on PU/PVDC blend reinforced with different types of cellulose nanocrystals. Mater. Renew. Sustain. Energy 7, 1–13. https://doi.org/10.1007/s40243-018-0128-6.
Yuwawech, K., Wootthikanokkhan, J., Wanwong, S., Tanpichai, S., 2017. Polyurethane/esterified cellulose nanocrystal composites as a transparent moisture barrier coating for encapsulation of dye sensitized solar cells. J. Appl. Polym. Sci. 134, 45010. https://doi.org/10.1002/app.45010.
Zhang, Y., Liu, M., Eperon, G.E., Leijtens, T.C., McMeekin, D., Saliba, M., Zhang, W., de Bastiani, M., Petrozza, A., Herz, L.M., Johnston, M.B., Lin, H., Snaith, H.J., 2015. Charge selective contacts, mobile ions and anomalous hysteresis in organic–inorganic perovskite solar cells. Mater. Horiz. 2, 315–322. https://doi.org/10.1039/C4MH00238E.
Zhang, Z., Song, F., Zhang, M., Chang, H., Zhang, X., Li, X., Zhu, X., Lü, X., Wang, Y., Li, K., 2019. Cellulose nanopaper with controllable optical haze and high efficiency ultraviolet blocking for flexible optoelectronics. Cellulose 26, 2201–2208. https://doi.org/10.1007/s10570-019-02253-y.
Zhao, X., Yan, G., Sun, Y., Tang, X., Zeng, X., Lin, L., Lei, T., 2019. Preparation of ethyl cellulose composite film with down conversion luminescence properties by doping

perovskite quantum dots. ChemistrySelect 4, 6516–6523. https://doi.org/10.1002/slct.201900822.
Zhi, J., Zhang, L.-Z., 2018. Durable superhydrophobic surface with highly antireflective and self-cleaning properties for the glass covers of solar cells. Appl. Surf. Sci. 454, 239–248. https://doi.org/10.1016/j.apsusc.2018.05.139.
Zhu, J., Tang, M., He, B., Shen, K., Zhang, W., Sun, X., Sun, M., Chen, H., Duan, Y., Tang, Q., 2021. Ultraviolet filtration and defect passivation for efficient and photostable CsPbBr 3 perovskite solar cells by interface engineering with ultraviolet absorber. Chem. Eng. J. 404, 126548 https://doi.org/10.1016/j.cej.2020.126548.